Gut

BVES regulates c-Myc stability via PP2A and suppresses colitis-induced tumorigenesis

Journal:	*Gut*
Manuscript ID	gutjnl-2015-310255.R2
Article Type:	Original Article
Date Submitted by the Author:	n/a
Complete List of Authors:	Parang, Bobak; Vanderbilt University, GI/Medicine Kaz, Andrew; University of Washington, GI/Medicince Barret, Caitlyn; Vanderbilt University, GI/Medicine Short, Sarah; Vanderbilt University, GI/Medicine Ning, Wei; Vanderbilt University, GI/Medicine Keating, Cody; Vanderbilt University, GI/Medicine Mittal, Mukul; Vanderbilt University, GI/Medicine Naik, Rishi; Vanderbilt University, GI/Medicine Washington, Mary; Vanderbilt University, Pathology Revetta, Frank; Vanderbilt University, Pathology Smith, Josh; Vanderbilt University, Surgical Sciences Chen, Xi; Vanderbilt, Biostatistics Wilson, Keith; Vanderbilt University, GI/Medicine; Vanderbilt University, GI/Medicine Brand, Thomas; Imperial College London, Developmental Dynamics Bader, David; Vanderbilt University, GI/Medicine Tansey, William; Vanderbilt, Cell and Developmental Biology Chen, Ru; University of Washington, GI/Medicince Brentnall, Teresa; University of Washington, GI/Medicince Grady, Bill; University of Washington, GI/Medicince Williams, Christopher; Vanderbilt, Medicine/GI
Keywords:	CANCER, IBD, ULCERATIVE COLITIS, COLONIC NEOPLASMS, COLORECTAL CANCER

BVES regulates c-Myc stability via PP2A and suppresses colitis-induced tumorigenesis

Short Title: BVES suppresses inflammatory carcinogenesis

Bobak Parang[1,2], Andrew M. Kaz[3,4], Caitlyn W. Barrett[1,2], Sarah P. Short[1,2], Wei Ning[1,2], Cody E. Keating[1,2], Mukul K. Mittal[1,2], Rishi D. Naik[1], Mary K. Washington[5], Frank L. Revetta[5], J. Joshua Smith[6], Xi Chen[8], Keith T. Wilson[1,2,8,9], Thomas Brand[10], David M. Bader[11], William P. Tansey[8,11], Ru Chen[4], Teresa A. Brentnall[4], William M. Grady[4,12], Christopher S. Williams[1,2,8,9]

[1]Department of Medicine, Division of Gastroenterology, Vanderbilt University; [2]Department of Cancer Biology, Vanderbilt University; [3]Research and Development Service, VA Puget Sound Health Care System; [4]Department of Medicine, Division of Gastroenterology, University of Washington, Seattle; [5]Department of Pathology, Microbiology, and Immunology, Vanderbilt University; [6]Department of Surgery, Vanderbilt University; [7]Department of Biostatistics, Vanderbilt University; [8]Vanderbilt Ingram Cancer Center; [9]Veterans Affairs Tennessee Valley Health Care System, Nashville, TN; [10]Department of Developmental Dynamics, Imperial College of London; [11]Department of Cell and Developmental Biology, Vanderbilt University; [12]Clinical Research Division, Fred Hutchinson Cancer Research Center

Keywords: Cancer, IBD, Ulcerative colitis, Colonic neoplasms, Colorectal cancer

Corresponding Author:
Christopher S. Williams, M.D., Ph.D.
Associate Professor of Medicine and Cancer Biology
Director, Physician Scientist Training Program
Staff Physician, VA Health System
Vanderbilt University School of Medicine
1065D MRB-IV
B2215 Garland Ave
Nashville, TN 37232

Disclosure of Potential Conflicts of Interest: The authors have no conflicts of interest to disclose.

Author Contributions: BP and **AMK** contributed equally to the work in the manuscript. **WMG** and **CSW** are co-corresponding authors. BP, AMK, CWB, and SPS developed the hypothesis, designed experiments, analyzed the data, and wrote the manuscript. BP, AMK, CWB, SPS, CEK, WN, MKM, RDN, FLR performed experiments. BP, AMK, CWB, SPS, MKW, JJS, XC, KTW, TAB, DMB, WPT, RC, TAB, WMG, CSW contributed to experimental design, generation of the reagents, and manuscript editing. BP, AMK, WMG, CSW conceived and supervised the project.

Word Count: 3788

ABSTRACT:

Objective: *Blood vessel epicardial substance* (BVES) is a tight junction-associated protein that regulates epithelial-mesenchymal states and is underexpressed in epithelial malignancy. However, the functional impact of BVES loss on tumorigenesis is unknown. Here we define the *in vivo* role of BVES in colitis-associated cancer (CAC), its cellular function, and its relevance to inflammatory bowel disease (IBD) patients.

Design: We determined *BVES* promoter methylation status using an Infinium HumanMethylation450 array screen of patients with ulcerative colitis with and without CAC. We also measured *BVES* mRNA levels in a tissue microarray consisting of normal colons and CAC samples. *Bves*$^{-/-}$ and wild-type mice (controls) were administered azoxymethane (AOM) and dextran sodium sulfate (DSS) to induce tumor formation. Lastly, we utilized a yeast two-hybrid screen to identify BVES interactors and performed mechanistic studies in multiple cell lines to define how BVES reduces c-Myc levels.

Results: *BVES* mRNA was reduced in tumors from patients with CAC via promoter hypermethylation. Importantly, *BVES* promoter hypermethylation was concurrently present in distant non-malignant appearing mucosa. As seen in human patients, *Bves* was underexpressed in experimental inflammatory carcinogenesis, and *Bves*$^{-/-}$ mice had increased tumor multiplicity and degree of dysplasia after AOM/DSS administration. Molecular analysis of *Bves*$^{-/-}$ tumors revealed Wnt activation and increased c-Myc levels. Mechanistically, we identified a new signaling pathway whereby BVES interacts with PR61α, a PP2A regulatory subunit, to mediate c-Myc destruction.

Conclusions: Loss of BVES promotes inflammatory tumorigenesis through dysregulation of Wnt signaling and the oncogene c-Myc. *BVES* promoter methylation status may serve as a CAC biomarker.

SUMMARY BOX

What is already known about this subject?

- Patients with ulcerative colitis are at greater risk for developing colon cancer.
- Blood vessel epicardial substance (BVES) is a tight junction protein that regulates epithelial-to-mesenchymal transition *in vitro.*
- c-Myc is an oncogene overexpressed in 50% of all malignancies, including colitis-associated cancer (CAC).
- **What are the new findings?**
- *BVES* promoter hypermethylation is present in CAC and distant uninvolved mucosa.
- *BVES* is underexpressed in patients with CAC compared to normal colonic tissue.
- Deletion of *Bves* promotes colitis-associated tumor multiplicity and dysplasia.
- BVES directs the PR61α-PP2A complex to target c-Myc for proteasomal destruction.

How might it impact on clinical practice in the foreseeable future?

- *BVES* promoter hypermethylation status is a potential biomarker to identify UC patients at risk for cancer.
- Our studies demonstrate a new mechanism for regulation of c-Myc, an oncogene that is dysregulated in numerous malignancies.
- BVES plays a key role in maintaining the integrity of the colonic mucosa and protecting from inflammatory carcinogenesis, and may represent a therapeutic target in CAC.

INTRODUCTION

Chronic inflammation promotes the development of colorectal cancer (**CRC**)[1,2]. Patients with inflammatory bowel disease (**IBD**), for example, have an elevated risk of developing CRC[3], particularly those who have extensive disease or long disease duration[4]. Although the pathogenesis of inflammatory carcinogenesis remains unclear, at least one component of malignant degeneration is thought to be disruption of intestinal epithelial function as a consequence of chronic inflammation[5,6]. Indeed, pathologic changes in adherens and tight junction proteins have been described in colitis and colitis-associated cancer (**CAC**)[6–8]. In addition to providing junctional integrity between cells, adherens and tight junctional complexes also transduce extracellular signals to direct intracellular programs ("outside-in" signaling[9]), such as those controlling cellular proliferation and differentiation. For example, E-cadherin can sequester β-catenin at the cell membrane, preventing its nuclear localization and transcriptional activity[10]. Given that dysregulation of junctional proteins commonly occurs in CAC, understanding their function in normal biology may yield clues to how their dysfunction promotes carcinogenesis.

Blood vessel epicardial substance (**BVES/POPDC1**) is a tight junction-associated protein often silenced in carcinomas secondary to promoter hypermethylation[11–13]. Restoring *BVES* expression in CRC cell lines promotes epithelial-like morphology and decreases proliferation, migration, invasion, xenograft tumor growth, and metastasis, together indicating broad regulatory capabilities[11]. Conversely, knockdown of *BVES* in epithelial-like cells induces a mesenchymal-like phenotype characterized by increased proliferation, altered morphology, and disorganized cell-cell contacts[11]. Yet how BVES

regulates these phenotypes is incompletely understood. Indeed, while several BVES interacting proteins have been identified[11], their known functions do not explain fully the role of BVES in maintaining epithelial phenotypes. Moreover, how BVES contributes to tumor development has not been tested using genetic approaches.

The transcription factor c-Myc is commonly overexpressed in cancer[14,15] and regulates proliferation, differentiation, apoptosis, and epithelial-to-mesenchymal transition[16]. In mouse models of sporadic CRC, decreased c-Myc levels reduce *Apc*-driven tumorigenesis[17]. In IBD, c-Myc is overexpressed in both inflamed tissues and CAC tumors[18], and network analysis of CAC samples indicated that c-Myc dysregulation functionally contributes to CAC progression[19]. c-Myc levels are also increased in experimental models of inflammatory carcinogenesis, such as the azoxymethane (**AOM**)/dextran sodium sulfate (**DSS**) mouse model of CAC[20]. Yet the processes responsible for c-Myc dysregulation in inflammatory carcinogenesis remain unidentified. To date, a complex network of proteins—including protein phosphatase 2A (PP2A), Axin1, and GSK3β—has been identified that regulates c-Myc protein levels by modifying the phosphorylation status of c-Myc at two residues, threonine 58 (**T58**) and serine 62 (**S62**)[21]. Ubiquitylation of c-Myc is initiated by phosphorylation at T58, leading to its ultimate degradation. Given the prominent role of c-Myc in driving oncogenic programs, understanding mechanisms that control PP2A dephosphorylation of c-Myc may identify new therapeutic targets in inflammatory carcinogenesis.

Here we report that BVES is an important regulator of inflammatory carcinogenesis programs and promotes c-Myc degradation through an interaction with the PR61α-PP2A complex. We observed that *BVES* is reduced in human CAC samples, and

further that the *BVES* promoter was hypermethylated within the tumors and at distant unaffected mucosa, suggesting a field effect. Using the AOM/DSS inflammatory carcinogenesis model, we determined that *Bves*$^{-/-}$ mice demonstrate greater tumor incidence and multiplicity as well as a higher degree of dysplasia and intratumoral proliferation. Furthermore, molecular analysis of *Bves*$^{-/-}$ tumors revealed increased c-Myc protein and signaling activity. c-Myc protein was also elevated in intestinal crypts from *Bves*$^{-/-}$ mice. In line with *in vivo* results, knockdown of BVES *in vitro* increased c-Myc stability and consequently increased expression of key c-Myc targets *ODC* and *CAD*. Conversely, BVES overexpression reduced c-Myc stability and increased c-Myc ubiquitylation. Using a yeast two-hybrid (**Y2H**) screen, we identified PR61α, the PP2A regulatory subunit critical for c-Myc degradation, as a BVES-interacting protein, and show that this interaction is required for BVES to modulate cellular c-Myc levels. Thus, we demonstrate that BVES coordinates PR61α-containing PP2A phosphatase complexes to restrict c-Myc protein levels and that BVES is a key suppressor of inflammatory carcinogenesis whose promoter methylation status may define patients with ulcerative colitis (**UC**) at risk for colon cancer.

MATERIALS AND METHODS

Mice, treatments, and analysis

AOM and DSS were prepared as previously described[22]. *Bves*$^{-/-}$ mice have been previously described[23]. Detailed protocols can be found in the **Supplementary Materials and Methods Section**.

BVES promoter methylation analysis

Tissue samples were obtained from colectomy specimens from individuals without UC, individuals with UC but without dysplasia or cancer, and UC patients with high-grade dysplasia and/or colon cancer. Clinical information is described in online **supplementary table 1.** Detailed protocols regarding epithelial isolation, methylation array, and pyrosequencing can be found in the **Supplementary Materials and Methods Section.**

See **Supplementary Materials and Methods** for detailed methods regarding cell culture experiments, RNA scope, promoter methylation analyses, and mouse analysis.

RESULTS

BVES is downregulated and its promoter is hypermethylated in CAC

As *BVES* is underexpressed via promoter hypermethylation in CRC[11], we asked whether the *BVES* promoter was also hypermethylated in CAC. Therefore, we analyzed *BVES* methylation status in an Infinium HumanMethylation450 array screen of IBD samples. The samples consisted of control patients (**Control—No UC**), patients with UC who did not have cancer (**UC—no HGD/CAC**), and two different types of samples from patients with UC who had colon cancer: the remote, non-malignant tissue (**UC—concurrent HGD/CAC**) and tissue with high-grade dysplasia and/or cancer (**HGD/CAC**). These analyses demonstrated that the *BVES* promoter was unmethylated in the controls–No UC (0.1% $\pm$ 0.016%), moderately methylated in UC–no HGD/CAC (16% $\pm$ 4.7%), and hypermethylated in the HGD/CAC among patients with colitis-associated carcinoma (HGD/CAC, 53% $\pm$ 2.6%) (**figure 1A**). Furthermore, remote non-neoplastic, mucosal samples (UC-Concurrent HGD/CAC) from the same patients who had CAC (HGD/CAC) were hypermethylated (50% $\pm$ 2.6%) to a similar degree as that observed in cancerous tissue. Interestingly, these results suggest that *BVES* promoter methylation may represent a field effect in CAC and that *BVES* promoter methylation status may identify UC patients with concurrent malignancy. To confirm the results derived from the HM450 methylation array studies, we pyrosequenced the *BVES* promoter in the same samples and again demonstrated low levels of methylation in the UC—no HGD/CAC cases, and higher methylation in both the UC—concurrent HGD/CAC and HGD/CAC cases (**figure 1B**).

It is possible that *BVES* promoter methylation, while increased, may not be sufficient to silence its expression. To determine whether *BVES* promoter methylation indeed reduced its transcription, we tested whether *BVES* mRNA was downregulated in CAC using high resolution *in situ* hybridization (RNAScope[24]) in a tissue microarray consisting of normal, UC, and CAC samples. *BVES* mRNA levels were low, but consistently present in normal colonic epithelial cells (**figure 1C**). In UC and CAC samples, however, *BVES* message was rarely detected and quantification of epithelial staining indicated a 5-fold decrease ($p<0.001$). Taken together, *BVES* RNA expression is downregulated in both UC and CAC, most likely due to promoter hypermethylation. Furthermore, as the *BVES* promoter is hypermethylated in both tumor and non-malignant mucosa in patients with CAC, *BVES* promoter methylation may serve as a biomarker associated with dysplasia or neoplasia in patients with IBD.

Bves loss promotes CAC development

While *BVES* underexpression was consistently observed in human CAC, these studies do not establish whether BVES loss actively promotes tumorigenesis. Therefore, we used mouse genetic approaches combined with the AOM/DSS model (**figure 2A**) to determine if BVES loss contributed to inflammatory tumorigenesis. While *Bves* was expressed at baseline in the murine colon at both the RNA and protein levels (see online **supplementary figure 1**), transcriptome profiling of AOM/DSS-induced tumors in WT mice showed a 5-fold decrease in *Bves* transcripts (**figure 2B**), mirroring the results observed in human CAC. As expected**,** we also observed changes in other tight junction constituents, supporting previous reports of tight junctional dysregulation in colitis and CAC[25]. We confirmed that *Bves* message was decreased in AOM/DSS tumor tissue by

qPCR in an independent sample set (**figure 2B**). Interestingly, *Bves* message also decreased in AOM/DSS treated non-malignant tissue compared to normal colons (**figure 2B**), again suggesting a field effect in inflammatory carcinogenesis. As a result, we hypothesized that complete loss of *Bves* might promote inflammatory carcinogenesis.

To test the effect of *Bves* loss in CAC, we compared WT and *Bves*$^{-/-}$ mice subjected to the same inflammatory carcinogenesis protocol. We first observed that *Bves*$^{-/-}$ mice lost a greater fraction of body weight compared to WT mice, most notably during cycle 3 (**figure 2C**), suggesting increased sensitivity to AOM/DSS treatment. Indeed, endoscopy one-week prior to sacrifice demonstrated increased tumor multiplicity in *Bves*$^{-/-}$ mice (**figure 2D)** and this was confirmed at necropsy where we observed 100% tumor penetrance in *Bves*$^{-/-}$ mice compared to 60% in WT mice (**figure 2E**). *Bves*$^{-/-}$ mice also demonstrated increased tumor multiplicity (6.5 ± 0.6 tumors per *Bves*$^{-/-}$ mouse vs. 2.2± 0.5 tumors per WT mouse, $p<0.001$), and tumor size (**figure 2E**). Furthermore, *Bves*$^{-/-}$ tumors exhibit more advanced dysplasia compared to WT tumors (**figure 2F**). Control mice treated with three cycles of DSS-only or a single AOM injection did not develop tumors during this time-frame (data not shown). Taken together, these results suggest that BVES underexpression in CAC functionally contributes to inflammatory carcinogenesis.

Increased proliferation and enhanced Wnt activation in *Bves*$^{-/-}$ tumors

To identify BVES-directed mechanisms responsible for modifying tumorigenesis, we examined proliferation and apoptosis in the tumors of AOM/DSS treated *Bves*$^{-/-}$ mice. Proliferation, as measured by phospho-histone H3 staining, was increased in *Bves*$^{-/-}$ tumors (**figure 3A**). Conversely, staining for cleaved caspase-3 indicated no difference in intratumoral apoptosis between *Bves*$^{-/-}$ and WT mice (**see online supplementary figure**

2). As Wnt activation can drive proliferation, we postulated that Wnt signaling might be perturbed in *Bves*$^{-/-}$ tumors. β-catenin dysregulation is a key indicator of hyperactive Wnt signaling[26], and β-catenin is also a mutational target in DMH/DSS inflammatory carcinogenesis, resulting in increased levels and altered subcellular distribution[27]. Therefore, we analyzed β-catenin by immunohistochemistry and observed excessive cytoplasmic and nuclear β-catenin localization in *Bves*$^{-/-}$ tumors compared to WT tumors (**figure 3B**). While these results suggested hyperactive Wnt signaling in *Bves*$^{-/-}$ tumors, we confirmed this by RNA-seq analysis, which indicated upregulation of established Wnt targets, such as *Mmp7, Wisp2,* and *Rspo4* (**figure 3C**), in *Bves*$^{-/-}$ tumors. Ingenuity Pathway Analysis (**IPA**)[28] of the RNA-seq data set also indicated hyperactive Wnt networks, such as *β-catenin* and *Tcf*. Finally, immunoblotting demonstrated greater expression of cyclin D1 and c-jun, two well-characterized Wnt target genes[29,30], in *Bves*$^{-/-}$ tumors (**figure 3D**). While previous experiments demonstrated that BVES could regulate Wnt signaling using *in vitro*, cell-based assays[11], these findings provide the first *in vivo* and genetic evidence supporting the hypothesis that BVES regulates Wnt activity.

BVES regulates c-Myc degradation

As c-Myc is a *bona-fide* Wnt transcriptional target[17], has been identified as a potential biomarker in patients with IBD at risk for CAC[19], and is overexpressed in AOM/DSS tumors[20], we postulated that c-Myc was dysregulated in *Bves*$^{-/-}$ tumors. Indeed, IPA analysis of intratumoral transcriptomes identified causal dysregulation[28] of c-Myc networks (**see online supplementary figure 3A**). While analysis of RNA-seq datasets showed only a modest increase in c-Myc transcripts in *Bves*$^{-/-}$ tumors compared to WT tumors (see online **supplementary figure 3B**), immunohistochemical staining for

c-Myc demonstrated an increase in both total c-Myc protein (**figure 4A**) and transcriptionally active, phosphorylated serine 62 c-Myc species in *Bves*$^{-/-}$ tumors (see online **supplementary figure 4**). Interestingly, immunoblotting in tumor-adjacent mucosa also showed higher c-Myc levels in *Bves*$^{-/-}$ colons, which suggested c-Myc was increased prior to tumor formation and that BVES might regulate c-Myc levels in the gut at baseline (**figure 4B**). To test this, we isolated crypts from untreated *Bves*$^{-/-}$ and WT mice and observed greater c-Myc protein in *Bves*$^{-/-}$ samples (**figure 4C**). Consistent with elevated c-Myc, qPCR for *Ornithine decarboxylase (Odc)*, a c-Myc transcriptional target, indicated a 4-fold increase in *Bves*$^{-/-}$ colons (see online **supplementary figure 5**). We also observed increased mRNA of c-Myc targets *Odc* and *E2f transcription factor 2 (E2f2)* (**figure 4D**) in "mini-gut" 3D cultures, demonstrating that BVES regulation of c-Myc activity was epithelial cell-autonomous.

As we observed increased c-Myc protein in *Bves*$^{-/-}$ tumors, we postulated that BVES could regulate c-Myc protein stability. Three cell lines—HEK 293T (non-malignant cell line), Caco2 (CRC cell line that can form a polarized epithelium), and HCE (Human Corneal Epithelial)—which all express BVES (**supplementary figure 6**)[11] were used for BVES knockdown experiments. In all three cell lines, *BVES* RNAi increased c-Myc protein levels (**figure 5A and supplementary figure 7**). In addition to increasing total c-Myc protein, we also observed that *BVES* knockdown reduced T58 phosphorylation, a key post-translational modification which signals for c-Myc degradation by the ubiquitin-proteasome system (**figure 5A**). This increase in c-Myc was functionally relevant as transcript levels of c-Myc targets *ODC* and *Carbamoyl-Phosphate Synthetase 2 Aspartate Transcarbamylase and Dihydroorotase* (*CAD*) were

increased with *BVES* knockdown (**figure 5B**). Furthermore, knockdown of BVES doubled c-Myc half-life compared to non-targeting control samples (**figure 5C**). Conversely, overexpressing BVES reduced c-Myc protein levels, increased T58 c-Myc species (**figure 5D**), dampened c-Myc transcriptional activation of the c-Myc responsive E2F2 reporter (**see online supplementary figure 8**), and decreased c-Myc protein half-life (**figure 5E**, lower panel). We then tested whether BVES could regulate c-Myc ubiquitylation, a central post-translational event targeting its destruction. Indeed, by overexpressing BVES we observed increased c-Myc polyubiquitylation (**figure 5F**). Moreover, inhibiting the proteasome using MG132 blocked BVES-induced reduction of c-Myc (**figure 5F**). Hence, our results suggest that BVES promotes the post-translational degradation of c-Myc.

BVES interacts with PR61α, PP2Ac, and c-Myc

To identify a molecular mechanism by which BVES orchestrates c-Myc degradation, we conducted a Y2H screen to define the BVES interactome. Characterization of this interactome using the PANTHER (Protein ANalysis THrough Evolutionary Relationships) Classification System[31] identified a number of biologic processes influenced by BVES (**figure 6A**). Interestingly, the screen identified that BVES interacted with four of the five members of the B' family of PP2A regulatory subunits (PPP2R5A, PPP2R5B, PPP2R5D, and PPP2R5E). PPP2R5A, also known as PR61α, is a key regulator of PP2A mediated c-Myc dephosphorylation. PR61α directs the heterotrimeric PP2A complex, consisting of a regulatory, catalytic, and structural subunit, to associate with doubly phosphorylated (T58/S62) c-Myc and dephosphorylate

S62, resulting in increased levels of monophosphorylated T58 c-Myc species, which signals c-Myc to be degraded by the proteaosome[32].

The BVES:PR61α interaction was then confirmed by directed Y2H (**figure 6A**) and by exogenous and endogenous co-immunoprecipitation in HEK 293T cells (**figure 6B and C**). If BVES were interacting with PR61α to promote c-Myc degradation, we hypothesized that BVES would complex with both the PP2A catalytic subunit (PP2Ac) and c-Myc, which we then demonstrated by co-immunoprecipitation (**figure 6D and E and see online supplementary figure 9**). We further used the proximity ligation assay (PLA) and confirmed interaction of both exogenous and endogenous BVES with endogenous PR61α and c-Myc (**figure 6F).** Overall, these data indicate that BVES complexes with c-Myc, PR61α, and the PP2A catalytic subunit.

BVES is essential for PR61α-mediated c-Myc degradation

PP2A dephosphorylation of S62 requires c-Myc to be phosphorylated at residue T58[33]. If BVES reduces c-Myc through PP2A, we reasoned c-Myc^{T58A}, a c-Myc mutant resistant to T58 phosphorylation, would escape BVES-induced degradation. Indeed, BVES expression consistently reduced c-Myc^{WT} but had no effect on c-Myc^{T58A} (**figure 7A**). We next hypothesized that knockdown of BVES would ablate PR61α-PP2A induced c-Myc degradation. Overexpression of PR61α reduced c-Myc protein subtly but consistently as previously reported[32] (**figure 7B**; compare lane 1 and 3). Knocking down BVES, however, rescued PR61α-induced degradation (**figure 7B**; compare lanes 3 and 4). We then tested whether BVES could enhance PR61α-mediated c-Myc degradation, and indeed, overexpression of BVES and PR61α substantially reduced c-Myc protein compared to PR61α or BVES alone (**figure 7C**; compare lane 4 to 2 or 3).

We then sought to determine whether BVES requires PR61α to degrade c-Myc. For these experiments we first mapped the BVES:PR61α interaction domain by serial deletions to the carboxy-terminus of BVES. Deleting the carboxy-terminal 30 residues, but not the last 15 residues, disrupted the BVES:PR61α interaction as demonstrated by Y2H and by co-IP, thus mapping the interaction domain to residues 330-345 (**figure 7D**). Importantly, this uncoupling mutant (BVES-330) demonstrated reduced affinity for c-Myc (**figure 7E**) and was unable to reduce c-Myc levels (**figure 7F**), indicating BVES indeed requires interaction with PR61α to regulate c-Myc. Overall, our results demonstrate that BVES, through PR61α, promotes c-Myc dephosphorylation, destabilization, and destruction, and thus provides mechanistic insight into one manner by which BVES may contribute to inflammatory carcinogenesis.

DISCUSSION

We, and others, have shown that BVES is underexpressed in gastrointestinal cancers and that restoration of BVES in cancer cell lines induces epithelial features. Here we provide the first genetic evidence that BVES modifies cancer phenotypes, as we demonstrate that mice lacking *Bves* have increased tumor multiplicity and dysplasia after establishment of inflammatory carcinogenesis. Further, we show *Bves*$^{-/-}$ tumors have increased c-Myc protein resulting in activation of c-Myc regulated networks. Moreover, we identify that BVES interacts with PR61α, a key regulatory subunit of the PP2A phosphatase complex, and promotes PP2A-mediated c-Myc dephosphorylation leading to c-Myc degradation. Uncoupling the BVES:PR61α interaction blocks BVES-dependent reduction of cellular c-Myc levels. To our knowledge, this is the first junctional-associated protein identified that regulates post-translational c-Myc status. The potential clinical relevance is demonstrated as we observed that *BVES* is downregulated in CAC likely secondary to promoter methylation. However, perhaps more importantly, we establish that the *BVES* promoter is also aberrantly methylated in distant, normal appearing tissues in patients with CAC/HGD—suggesting a field effect. Thus, our findings not only reveal that deletion of BVES promotes CAC, but also that *BVES* promoter methylation status may be a clinically important surrogate marker of colitis-associated dysplasia or CAC in IBD patients.

Chronic colitis has been shown to accelerate genome-wide methylation changes[34]; it has been hypothesized that this greater rate of methylation contributes to the increased cancer risk in patients with colitis by silencing tumor suppressors. Understanding how methylation broadly affects inflammatory tumorigenesis is important to design therapies

and screening strategies for IBD patients. Our report specifically identifies that the *BVES* promoter is hypermethylated in UC patients who have CAC. Interestingly, *BVES* promoter hypermethylation is observed not only in the cancerous tissue, but also in the non-malignant mucosa in these patients. Currently, the standard method of cancer screening in IBD patients, who are at up to a 10-fold elevated risk of developing CAC[1], is surveillance colonoscopy performed with the hope that cancer will be detected at an early, treatable stage. Yet the detection of neoplasia in the colon can be challenging in individuals with IBD, as the lesions are frequently flat and difficult to detect in a background of acute and chronic inflammatory changes. Our data suggest that aberrant *BVES* promoter methylation may be a useful biomarker for the presence of CAC, or even dysplasia, and that measuring *BVES* promoter methylation status could serve as a clinically useful tool to identify patients at risk for colon dysplasia or cancer.

While the molecular pathogenesis of CAC remains incompletely understood, recent work has shown the importance of NF-κB signaling[35], the intestinal microbiota[36], the tumor microenvironment[37], and the innate immune system[38] in regulating inflammatory tumorigenesis. A growing body of evidence also supports the important role of epithelial junctional constituents in inflammation and CRC. For example, mice expressing a dominant negative N-cadherin display disrupted adherens junctions and develop severe inflammation and colitis-associated dysplasia[39]. Likewise, knocking out *Junctional adhesion molecule* (*Jam-A*) results in a dramatic increase in susceptibility to DSS-induced colitis[8]. Here we show that deletion of *Bves*, a tight junction-associated protein, augments inflammatory carcinogenesis. Indeed, loss of BVES appears to increase tumor initiation and progression. We postulate that this is likely due to dual

regulation of Wnt signaling and c-Myc protein degradation. Our results further strengthen the concept that junctional constituents are important regulators of colitis-induced tumor initiation and progression.

In the last decade, BVES has been shown to regulate a variety of cellular processes. For example, a Y2H screen of a mouse heart library identified an interaction between BVES and GEFT, a guanine nucleotide exchange factor[40]. Indeed, it was shown that expression of BVES modulated cell shape and locomotion, thus linking BVES to Rho-family GTPase signaling[40]. BVES has also been shown, via an interaction with ZO-1, to regulate GEF-H1-mediated RhoA activity[11]. More recently, it was reported that BVES plays a regulatory role in cardiac pacemaking through binding of cAMP and interacting with potassium channel TREK-1[41]. Further, BVES interacts with CAV3, a caveolin expressed in the muscle tissue, and cardiac myocytes in *Bves*$^{-/-}$ mice have altered calveolar number and size[42]. Thus, BVES, through scaffolding with protein complexes, regulates a wide variety of basic, yet essential, cellular processes.

Our results now expand the known regulatory roles of BVES to include maintaining appropriate c-Myc protein levels. We show that BVES, through its interaction with the PR61α-containing PP2A phosphatase complex, can promote c-Myc degradation and that silencing BVES prevents PR61α-induced degradation of c-Myc. Moreover, mutating BVES so that it is unable to associate with PR61α renders BVES unable to initiate c-Myc destruction. The post-translational regulation of c-Myc requires coordination of numerous proteins to modify its phosphorylation and ubiquitylation status[21]. Precisely how BVES coordinates the PR61α-PP2A complex remains to be understood, but given that analysis of BVES structure shows no apparent enzymatic

motifs in BVES, it is likely that BVES acts as a scaffold allowing for complex formation, similar to AXIN1[21]. Interestingly, in addition to the membranous staining of the BVES:PR61α complex, there also appears to be peri-nuclear and cytoplasmic localization (**figure 6F**), which is consistent with previous reports describing the dynamic subcellular localization of BVES and its family members[43]. The PP2A family has been associated with tight junctional complexes regulating cellular permeability, but their exact role remains controversial[44]. BVES may bridge PP2A complexes to tight junctions and our report adds a new molecular mechanism for "outside-in" signaling in the epithelium.

Because c-Myc regulates thousands of genes, even subtle changes in c-Myc expression can have profound effects on cellular transcriptomes that promote tumorigenesis[45]. Indeed, strict regulation of c-Myc is an important component of homeostasis, and this is particularly true in the intestine. Acute expression of c-Myc, for example, dramatically expands the intestinal crypts and results in loss of differentiated cells[46]. Moreover, it has been shown that c-Myc is essential for *Apc*-mediated intestinal tumorigenesis[17]. Thus, BVES may serve as an important suppressor of inflammatory tumorigenesis via attenuating excessive c-Myc levels. More broadly, BVES could act as a regulator of c-Myc in a variety of tissues, as BVES is expressed in most epithelial tissues, such as lung, stomach, and breast, and its downregulation or promoter hypermethylation has been documented in diverse epithelium[11–13].

Taking our data together, one can envision a model in which chronic inflammation leads to *BVES* promoter hypermethylation, resulting in suppression of *BVES* transcription and reduced cellular protein levels. Loss of BVES impairs PR61α

directed PP2A dephosphorylation of c-Myc, thus favoring increased cellular pools of c-Myc, a potent oncogene, likely, in cooperation with other oncogenic events, contributing to tumor progression (**figure 8**).

ACKNOWLEDGEMENTS:

We would like to thank the members of the Williams lab who helped discuss and review the manuscript. We would also like to thank Dr. Brian Grieb and Dr. Joseph Roland for their helpful suggestions. Finally, we appreciate the advice and counsel from Dr. R. Daniel Beauchamp and Dr. Barbara Fingelton in preparing the manuscript.

REFERENCES

1. A, Mantovani A, Allavena P, et al. Cancer-related inflammation. Nature 2008;454(7203):436–44.
2. Danese S, Mantovani A. Inflammatory bowel disease and intestinal cancer: a paradigm of the Yin-Yang interplay between inflammation and cancer. Oncogene 2010;29(23):3313–3323.
3. Terzić J, Grivennikov S, Karin E, et al. Inflammation and colon cancer. Gastroenterology 2010;138(6):2101–2114.e5.
4. Jess T, Simonsen J, Jørgensen KT, et al. Decreasing risk of colorectal cancer in patients with inflammatory bowel disease over 30 years. Gastroenterology 2012;143(2):375–81.
5. Schmitz H, Barmeyer C, Fromm M, et al. Altered tight junction structure contributes to the impaired epithelial barrier function in ulcerative colitis. Gastroenterology 1999;116(2):301–309.
6. Gibson P, Rosella O, Nov R, et al. Colonic epithelium is diffusely abnormal in ulcerative colitis and colorectal cancer. Gut 1995;36(6):857–863.
7. Karayiannakis AJ, Syrigos KN, Efstathiou J, et al. Expression of catenins and E-cadherin during epithelial restitution in inflammatory bowel disease. J Pathol 1998;185(4):413–418.
8. Vetrano S, Rescigno M, Rosaria Cera M, et al. Unique role of junctional adhesion molecule-A in maintaining mucosal homeostasis in inflammatory bowel disease. Gastroenterology 2008;135(1):173–184.
9. Severson EA, Parkos CA. Mechanisms of outside-in signaling at the tight junction by junctional adhesion molecule A. Ann N Y Acad Sci 2009;1165:10–18.
10. Orsulic S, Huber O, Aberle H, et al. E-cadherin binding prevents β-catenin nuclear localization and β-catenin / LEF- 1-mediated transactivation. J Cell Sci 1999;1245:1237–1245.
11. Williams CS, Zhang B, Smith JJ, et al. BVES regulates EMT in human corneal and colon cancer cells and is silenced via promoter methylation in human colorectal carcinoma. J Clin Invest 2011;121(10):4056–4069.
12. Feng Q, Hawes SE, Stern JE, et al. DNA methylation in tumor and matched normal tissues from non-small cell lung cancer patients. Cancer Epidemiol Biomarkers Prev 2008;17(3):645–654.

13. Kim M, Jang HR, Haam K, et al. Frequent silencing of popeye domain-containing genes, BVES and POPDC3, is associated with promoter hypermethylation in gastric cancer. Carcinogenesis. 2010;31(9):1685–1693.

14. Toon CW, Chou A, Clarkson A, et al. Immunohistochemistry for Myc predicts survival in colorectal cancer. PLoS One 2014;9(2):e87456.

15. Koo SH, Kwon KC, Shin SY, et al. Genetic alterations of gastric cancer: comparative genomic hybridization and fluorescence in situ hybridization studies. Cancer Genet Cytogenet 2000;117(2):97–103.

16. Cowling VH, Cole MD. E-cadherin repression contributes to c-Myc-induced epithelial cell transformation. Oncogene 2007;26(24):3582–3586.

17. Yekkala K, Baudino TA. Inhibition of intestinal polyposis with reduced angiogenesis in ApcMin/+ mice due to decreases in c-Myc expression. Mol Cancer Res 2007;5(12):1296–1303.

18. Ciclitira PJ, Macartney JC, Evan G. Expression of c-myc in non-malignant and pre-malignant gastrointestinal disorders. J Pathol 1987;151(4):293–296.

19. Brentnall TA, Pan S, Bronner MP, et al. Proteins that underlie neoplastic progression of ulcerative colitis. Proteomics - Clin Appl 2009;3(11):1326–1337.

20. Suzuki R, Miyamoto S, Yasui Y, et al. Global gene expression analysis of the mouse colonic mucosa treated with azoxymethane and dextran sodium sulfate. BMC Cancer 2007;7:84.

21. Arnold HK, Zhang X, Daniel CJ, et al. The Axin1 scaffold protein promotes formation of a degradation complex for c-Myc. EMBO J 2009;28(5):500–512.

22. Barrett CW, Fingleton B, Williams A, et al. MTGR1 is required for tumorigenesis in the murine AOM/DSS colitis-associated carcinoma model. Cancer Res 2011;71(4):1302–1312.

23. Andrée B, Fleige A, Arnold HH, et al. Mouse Pop1 is required for muscle regeneration in adult skeletal muscle. Mol Cell Biol 2002;22(5):1504–1512.

24. Wang F, Flanagan J, Su N, et al. RNAscope: A novel in situ RNA analysis platform for formalin-fixed, paraffin-embedded tissues. J Mol Diagnostics 2012;14(1):22–29.

25. Weber CR, Nalle SC, Tretiakova M, et al. Claudin-1 and claudin-2 expression is elevated in inflammatory bowel disease and may contribute to early neoplastic transformation. Lab Invest 2008;88(10):1110–1120.

26. Korinek V, Barker N, Morin PJ, et al. Constitutive transcriptional activation by a beta-catenin-Tcf complex in APC-/- colon carcinoma. Science 1997;275(5307):1784–1787.

27. Kohno H, Suzuki R, Sugie S, et al. B-catenin mutations in a mouse model of inflammation-related colon carcinogenesis induced by 1,2-dimethylhydrazine and dextran sodium sulfate. Cancer Sci 2005;96(2):69–76.

28. Krämer A, Green J, Pollard J, et al. Causal analysis approaches in Ingenuity Pathway Analysis. Bioinformatics 2014;30 (4): 523-530.

29. Tetsu O, McCormick F. Beta-catenin regulates expression of cyclin D1 in colon carcinoma cells. Nature 1999;398(6726):422–426.

30. Mann B, Gelos M, Siedow Q, et al. Target genes of beta-catenin-T cell-factor/lymphoid-enhancer-factor signaling in human colorectal carcinomas. Proc Natl Acad Sci U S A 1999;96(4):1603–1608.

31. Mi H, Muruganujan A, Thomas PD. PANTHER in 2013: Modeling the evolution of gene function, and other gene attributes, in the context of phylogenetic trees. Nucleic Acids Res 2013;41(D1):D377–86.

32. Arnold HK, Sears RC. Protein Phosphatase 2A regulatory subunit B56α associates with c-Myc and negatively regulates c-Myc accumulation protein. Mol Cell Biol 2006;26(7):2832–2844.

33. Yeh E, Cunningham M, Arnold H, et al. A signalling pathway controlling c-Myc degradation that impacts oncogenic transformation of human cells. Nat Cell Biol 2004;6(4):308–318.

34. Issa JJ, Ahuja N, Toyota M. Accelerated age-related CpG island methylation in ulcerative colitis. Cancer Res 2001:3573–3577.

35. Grivennikov S, Karin E, Terzic J, et al. IL-6 and Stat3 are required for survival of intestinal epithelial cells and development of colitis-associated cancer. Cancer Cell 2009;15(2):103–113.

36. Arthur JC, Perez-Chanona F, Muhlbauger M, et al. Intestinal inflammation targets cancer-inducing actvity of the microbiota. Science 2012; 338 (6103); 120-123.

37. Katoh H, Wang D, Daikoku T, et al. CXCR2-expressing myeloid-derived suppressor cells are essential to promote colitis-associated tumorigenesis. Cancer Cell 2013;24(5):631–644.

38. Fukata M, Chen A, Vamadevan AS, et al. Toll-like receptor-4 promotes the development of colitis-associated colorectal tumors. Gastroenterology 2007;133(6):1869–81.

39. Hermiston ML, Gordon JI. Inflammatory bowel disease and adenomas in mice expressing a dominant negative N-Cadherin. Science 1995;270(5239):1203–1207.

40. Smith TK, Hager H, Francis R, et al. Bves directly interacts with GEFT, and controls cell shape and movement through regulation fo Rac1/Cdc42 activity. Proc Natl Acad Sci U S A 2008;105(24): 8298-8303.

41. Froese A, Breher SS, Waldeyer C, et al. Popeye domain containin proteins are essential for stress-mediated modulation of cardiac pacemaking in mice. J Clin Invest 2012;122(3):1119-1130.

42. Alcalay Y, Hochhauser E, Kliminski V, et al. Popeye domain containing 1 (Popdc1/Bves) is a caveolae-associated protein involved in ischemia tolerance. PLoS One 2013;8(9):e71100.

43. Osler ME, Chang MS, Bader DM. Bves modulates epithelial integrity through an interaction at the tight junction. J Cell Sci 2005;118(20):4667–4678.

44. Dunagan M, Chaudhry K, Samak G, et al. Acetaldehyde disrupts tight junctions in Caco-2 cell monolayers by a protein phosphatase 2A-dependent mechanism. AJP Gastrointest Liver Physiol 2012;303(12):G1356–64.

45. Kim J, Woo AJ, Chu J, et al. A Myc network accounts for similarities between embryonic stem and cancer cell transcription programs. Cell 2010;143(2):313–324.

46. Finch AJ, Soucek L, Junttila MR, et al. Acute overexpression of Myc in intestinal epithelium recapitulates some but not all the changes elicited by Wnt/beta-catenin pathway activation. Mol Cell Biol 2009;29(19):5306–5315.

Legends

Figure 1 A field effect of *BVES* promoter hypermethylation in colitis-associated cancer.

(A) Average *BVES* promoter methylation status in the indicated sample from the Infinium HumanMethylation 450 Array. Methylation was measured in four sample types: colon epithelia from patients who did not have UC (Control—No UC); colon epithelia from UC patients who did not have dysplasia or carcinoma (UC—no HGD/CAC); non-malignant colon epithelia from UC patients (UC—concurrent HGD/CAC) and malignant colon epithelia (HGD/CAC) from UC patients who had dysplasia/carcinoma. Control—No UC, n=17; UC—no HGD/CAC, n=11; UC—concurrent HGD/CAC, n=10; HGD/CAC, n=10. **p<0.01.

(B) Pyrosequencing at four sequential CpG dinucleotides in the *BVES* promoter. Each shape represents a separate individual, with mean methylation values depicted with black bars. ***p<0.001.

(C) Representative images of high-resolution in situ (RNAscope™) analysis of *BVES* message in normal colons (n=11), UC (n=13), and CAC (n=19). Right: Quantification of *BVES* expressing epithelial cells per tissue microarray core. Size standard=50 microns. ***p<0.001

Figure 2 BVES modifies inflammatory carcinogenesis.

(A) Schematic of AOM/DSS protocol and timeline. Mice were injected with 7.5 mg/kg of AOM and treated with 2.5% DSS at the indicated time.

(B) Left: Heat map of RNA-seq data derived from WT colons (n=3) and WT AOM/DSS tumors (n=3). Red indicates genes increased and green indicates genes decreased in

tumors compared to normal colon. Right: qPCR of *Bves* message levels in normal colons (Normal, n=5), non-malignant AOM/DSS treated colon (NM, n=5) and AOM/DSS tumor (Tumor, n=6). Tissue harvested from WT mice after AOM/DSS treatment. ***p<0.001.

(C) Weights of *Bves*$^{-/-}$ and WT mice during AOM/DSS treatment. Weights are presented as fraction of initial weight. *Bves*$^{-/-}$ (male: n=8, female: n=7) and WT (male: n=5, female: n=10). *p<0.05, ***p<0.01, ***p<0.001.

(D) Representative colonoscopy images of WT and *Bves*$^{-/-}$ colons after the second cycle of DSS treatment. Right: Quantification of tumor multiplicity by endoscopy assessment.

(E) Tumor incidence, multiplicity, and size distribution at necropsy in WT and *Bves*$^{-/-}$ mice. Blue = female mice, black = male mice.*p<0.05, ***p<0.001.

(F) Left: Representative H&E stained sections demonstrating the histologic features of WT and *Bves*$^{-/-}$ tumors. Size standard=100 microns. Right: Blinded histological scoring of degree of dysplasia of tumors from WT and *Bves*$^{-/-}$ mice. Graph represents percentage of mice with intratumoral low or high-grade dysplasia.

Figure 3 Dysregulated Wnt signaling in *Bves*$^{-/-}$ tumors.

(A) Left: Representative images of phospho-histone H3 (pH3) immunohistochemistry in WT and *Bves*$^{-/-}$ tumors. Size standard=50 microns. Right: Quantification of pH3 positive cells per tumor high power field (HPF). Data is presented as the mean number of positive cells per tumor HPF per mouse. At least five HPF per mouse were scored. Student's t test, *p<0.05.

(B) Left: H&E stained sections, size standard=50 microns. Middle: Representative images of β-catenin immunohistochemistry, low magnification, size standard=50

microns. Right: β-catenin immunohistochemistry, high magnification, size standard=20 microns. Far right: Quantification of intratumoral β-catenin immunohistochemistry. An index was employed to quantify extent of nuclear and cytoplasmic β-catenin staining. This index is generated by multiplying the staining intensity (on a scale of 100-500) by percentage of the cells demonstrating nuclear staining. For example, a score of 500 indicates a field that demonstrated very intense nuclear β-catenin stain while a score of 100 indicates a field that has weak nuclear β-catenin staining. Data is presented as the mean score per tumor HPF per mouse. At least five HPF per mouse were scored.

(C) Wnt target genes upregulated in *Bves*$^{-/-}$ tumors identified in RNA-seq dataset (WT, n=3; *Bves*$^{-/-}$, n=3).

(D) Immunoblot of Cyclin D1 and c-jun in *Bves*$^{-/-}$ and WT tumors. β-actin was used as a loading control.

Figure 4 c-Myc signaling is dysregulated in *Bves*$^{-/-}$ mice in inflammatory carcinogenesis. (A) Left: Representative images of immunohistochemistry for intratumoral c-Myc. Right: quantification of c-Myc positive cells per tumor high power field (HPF). HPFs were scored according to an index from 1-4 (a score of 1 denotes less than 25% of positive cells per HPF; a score of 2 denotes 25-50%; a score of 3 denotes 50-75%; a score of 4 denotes 80-100%). Data is presented as the mean score per tumor HPF per mouse. At least five HPF per mouse were scored. Student's t test, *$p<0.05$. Size standard=50 microns

(B) Immunoblot of c-Myc in WT and *Bves*$^{-/-}$ normal adjacent colons. Blots were imaged using the LiCor Odyssey system and quantified using Image Studio analysis. Student's t test, $p<0.05$.

(C) Immunoblot of c-Myc in WT (n=3) and *Bves*$^{-/-}$ (n=3) intestinal crypts.

(D) qPCR for *Odc* and *E2f2* in enteroid cultures Student's t test, *$p<0.05$.

In all western blots, β-actin served as loading control.

Figure 5 BVES regulates c-Myc stability and activity.

(A) c-Myc and T58 phospho-c-Myc protein levels after *BVES* knockdown in HEK 293T (left) or Caco2 (right) cells after 48 hr serum starvation.

(B) qRT-PCR assay for c-Myc targets *ODC* and *CAD* following *BVES* knockdown in the indicated cell lines. Data are presented as mean ±SEM and in triplicates. *$p<0.05$, **$p<0.01$.

(C) Cycloheximide treatment (100 μg/ml) of HEK 293T cells with and without *Bves* knockdown followed by immunoblotting for c-Myc.

(D) c-Myc and T58 phospho-c-Myc protein levels after overexpression of V5:BVES in HEK 293T cells.

(E) HEK 293T cells co-transfected with HA:c-Myc and V5:BVES were then treated with cycloheximide (100 μg/ml) followed by immunoblotting for the indicated protein.

(F) Left: His:Ubiquitin and HA:c-Myc were co-transfected into HEK 293T cells along with V5:BVES. Cells were treated with proteasome inhibitor MG132 (20 μm) for 4 hours before His:Ubiquitin complexes were immunoprecipitated and resolved by SDS-PAGE. Ubiquitylated HA:c-Myc complexes were visualized by immunoblotting (Ub-c-Myc). Total ubiquitylated protein (Total ub) was examined as a control. Right: HEK 293T cells

co-transfected with HA:c-Myc and V5:BVES were treated with proteasome inhibitor MG132 (20 μm) for 4 hours. Whole cell lysates were analyzed for HA:c-Myc expression. In all immunoblots, β-actin was used as a loading control. All experiments were replicated three times.

Figure 6 BVES interacts with PR61α, PP2A, and c-Myc.

(A) PANTHER Biologic Process Analysis of BVES interactome. Inset: Directed yeast two-hybrid of BVES and PR61α.

(B) Co-immunoprecipitation of exogenous and (**C**) endogenous PR61α:BVES complexes in HEK 293T cells.

(D) Co-immunoprecipitation of V5:BVES and HA:PP2Ac or (**E**) HA:c-Myc.

(F) Left: Proximity ligation assay in HEK 293T cells transfected with V5:BVES. Left: control, middle: α-PR61α, right: α-c-Myc. Right: Proximity ligation assay in HEK 293T cells for endogenous protein interactions. Left: control, middle: α-PR61α, right: α-c-Myc. Anti-HA was used as a control in both exogenous and endogenous localization. Scale bar denotes 10 μm. Red staining is positive signal from the PLA interaction, and blue staining is DAPI. In all immunoblots blots, β-actin was used to ensure loading consistency. All experiments were repeated at least two times.

Figure 7 The BVES:PR61α interaction is required to promote c-Myc degradation.

(A) WT HA:c-Myc or phospho-mutant HA:T58A c-Myc levels after either empty vector (negative control) or V5:BVES transfection in HEK 293T cells.

(B) Immunoblotting for HA:c-Myc levels following PR61α overexpression in the setting of BVES knockdown or (**C**) when both PR61α and BVES are present HEK 293T cells. **(D)** Top: Mapping the PR61α BVES binding interface via directed yeast two-hybrid (Full length BVES, residues 1-345, 1-330, 1-302, negative control (Neg Ctrl), and positive control (Pos Ctrl)). Below: Co-immunoprecipitation of the indicated BVES mutants and PR61α in HEK 293T cells..

(**E**) Co-immunoprecipitation of the indicated BVES mutants and HA:c-Myc in HEK 293T cells.

(F) HA:c-Myc protein levels after transfection of the indicated BVES construct in HEK 293T cells.

In all immunoblots, β-actin was used as a loading control. All experiments were repeated at least two times.

Figure 8 Working model of the role of BVES in regulating c-Myc degradation and colitis-associated cancer development.

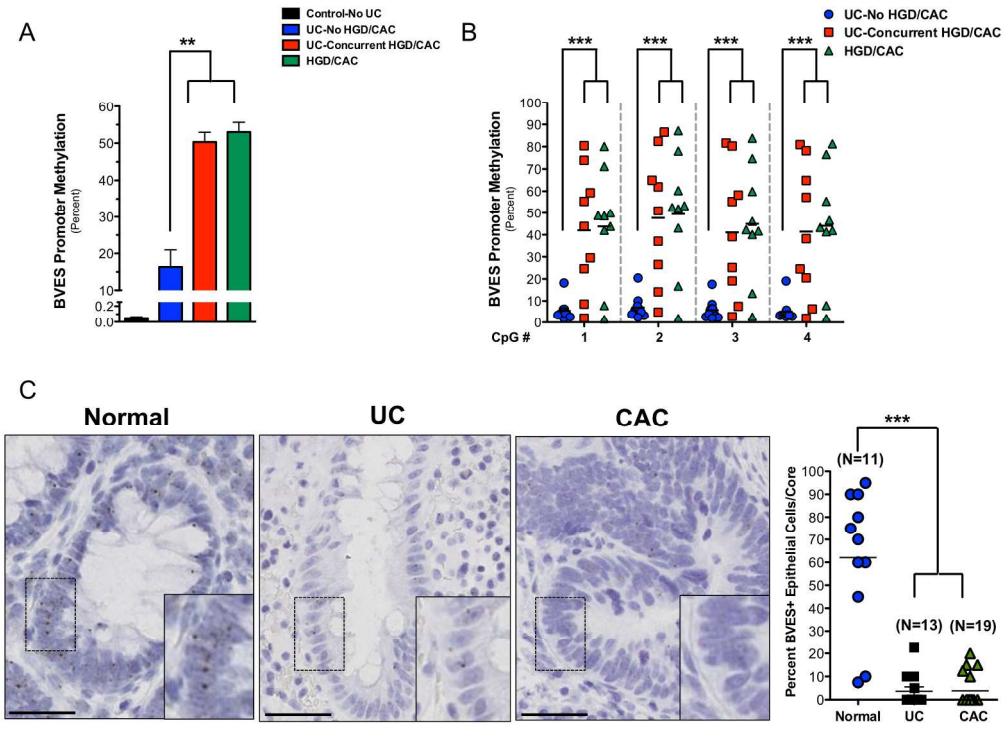

254x190mm (300 x 300 DPI)

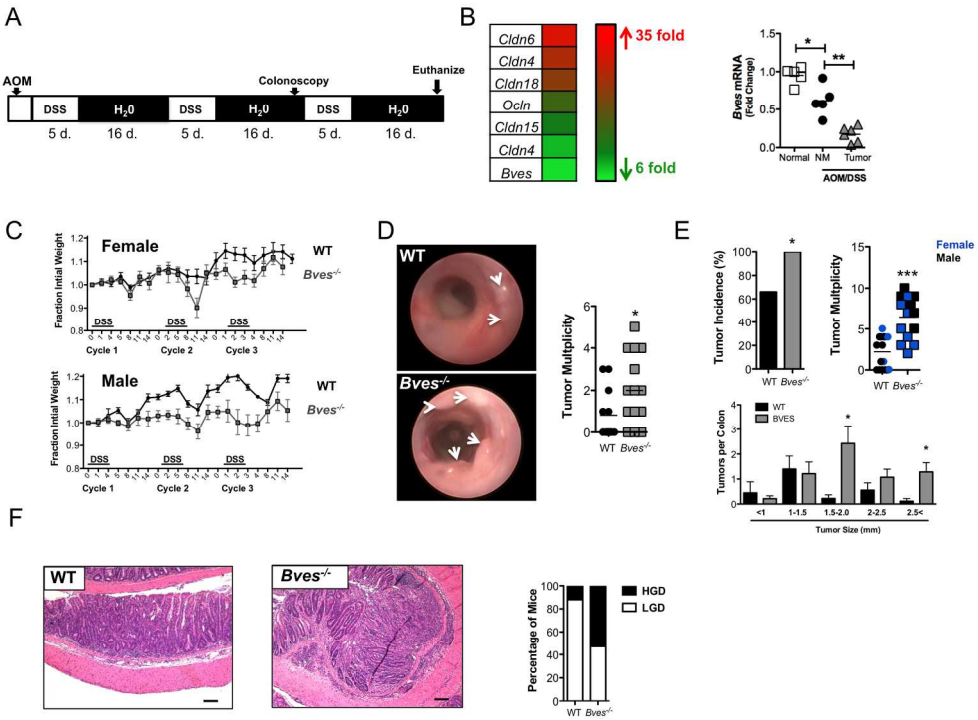

Figure 2
182x137mm (300 x 300 DPI)

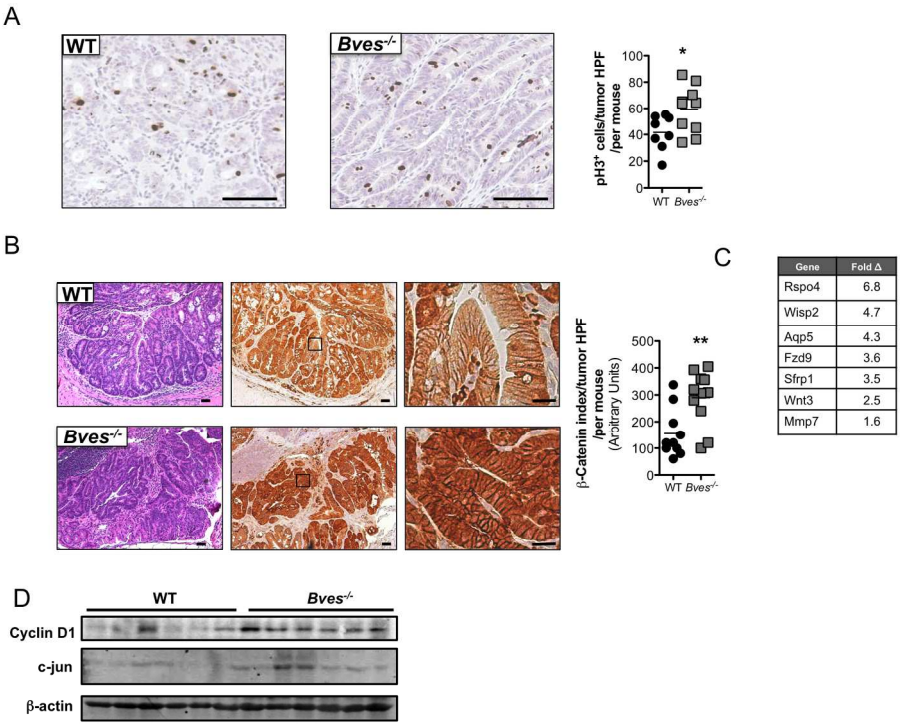

Figure 3
182x137mm (300 x 300 DPI)

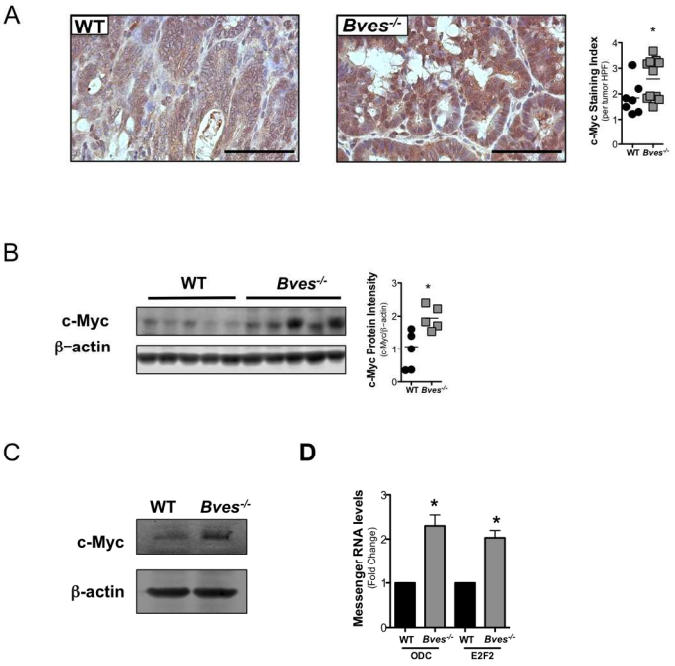

Figure 4
182x137mm (300 x 300 DPI)

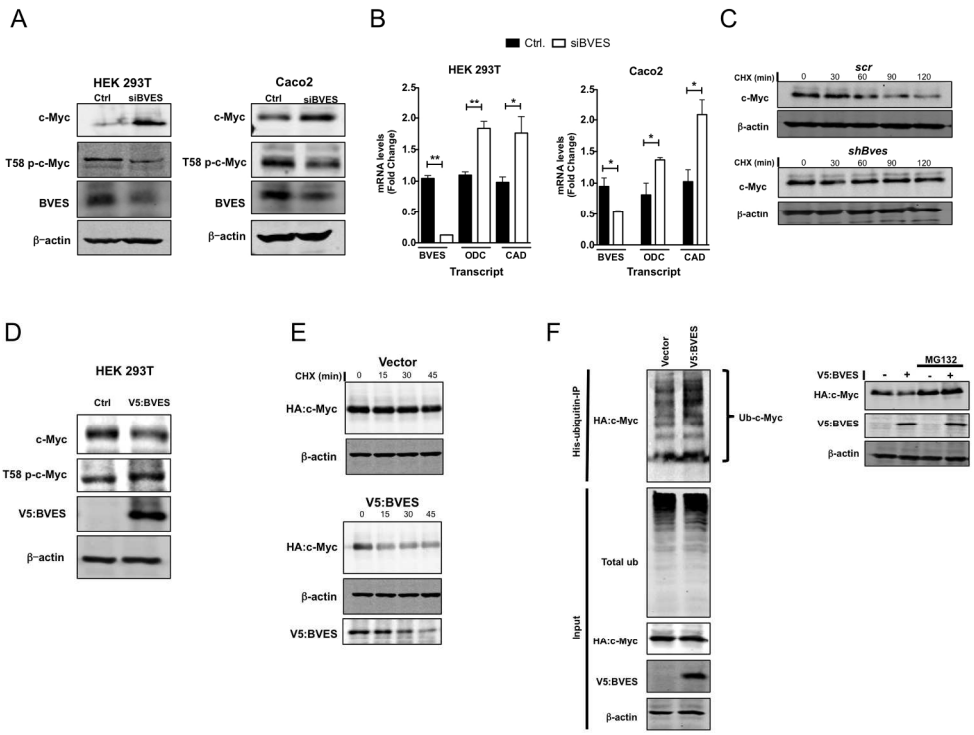

Figure 5
182x137mm (300 x 300 DPI)

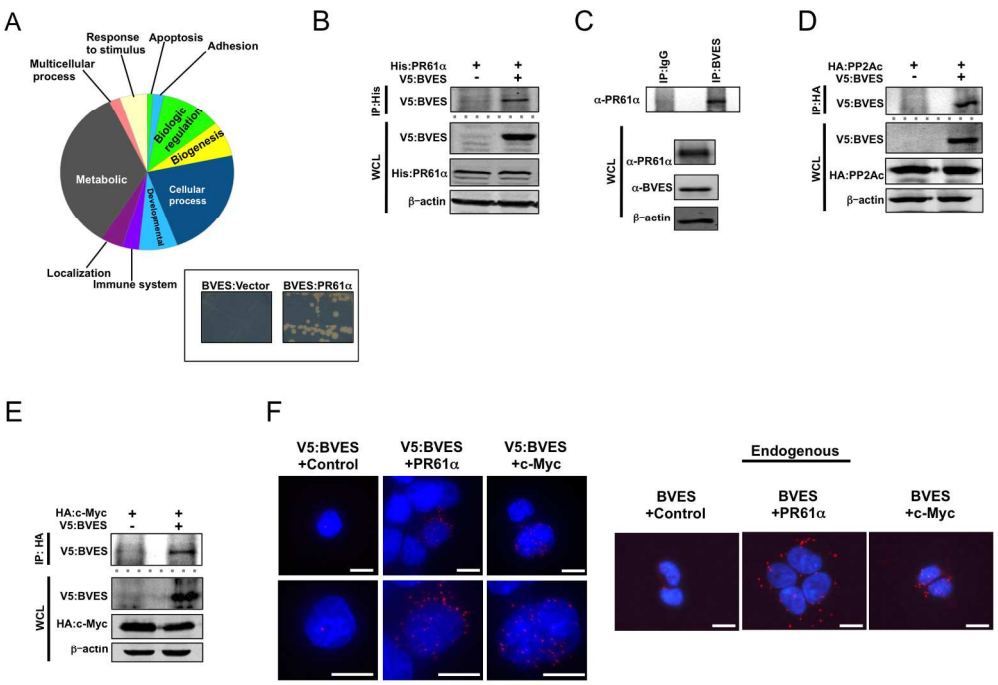

Figure 6
182x137mm (300 x 300 DPI)

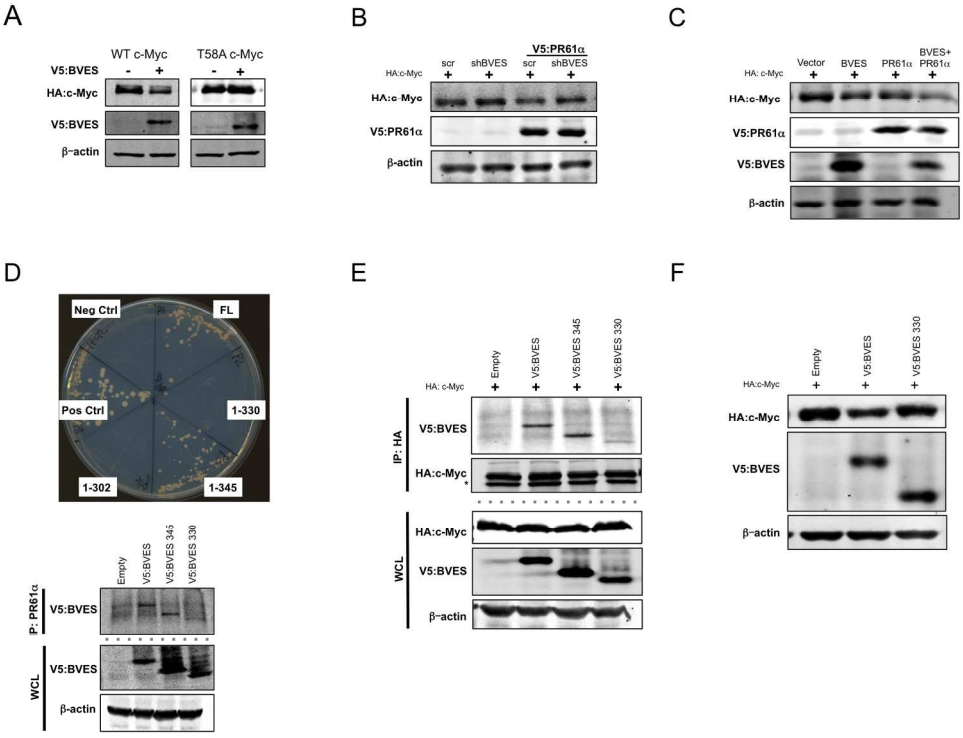

Figure 7
182x137mm (300 x 300 DPI)

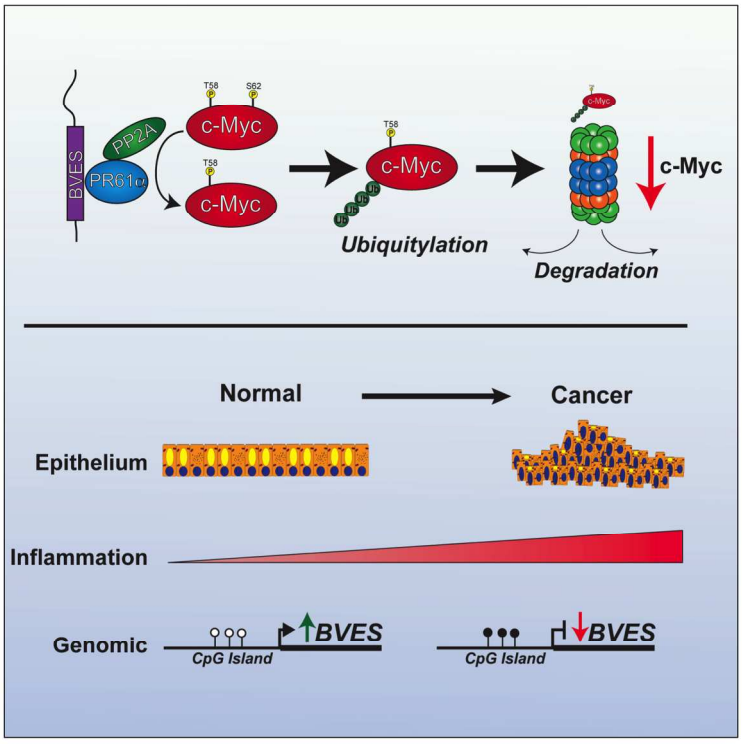

Figure 8
182x137mm (300 x 300 DPI)

SUPPLEMENTARY MATERIALS AND METHODS

Mice, treatment, and analysis

Over the course of two experiments, 15 wildtype (10 female and 5 male) (WT) C57BL/6 and 15 *Bves*$^{-/-}$ (7 female and 8 male) mice were treated with 7.5 mg/kg of AOM by intraperitoneal injection and placed on 3 cycles of 5 day treatments with 2.5% DSS. Mice were between 8-12 weeks of age before AOM treatment. All mice were bred and housed in the same facility throughout the duration of the experiment. Both WT and *Bves*$^{-/-}$ pure C57BL/6 colonies were maintained in the same room for a year prior to beginning the experiment to ensure a controlled microenvironment. *Bves*$^{-/-}$ mice were previously characterized[1]. All *in vivo* procedures were carried out in accordance with protocols approved by the Vanderbilt Institutional Animal Care and Use Committee.

After the mice were sacrificed, colons were irrigated with phosphate-buffered saline (PBS). The colons were then opened longitudinally and rolled orienting the most distal region of the colon such that it was located in the innermost part of the roll. The tissues were then fixed in formalin (1:10 dilution buffered) overnight. The solution was subsequently changed to 70% ethanol before standard paraffin-embedding. Five micron sections were cut and stained with hematoxylin and eosin (H&E) by the Vanderbilt Translational Pathology Shared Resource Core. Proliferation was measured by phospho-histone H3 (pH3) staining using anti-pH3 at 1:150 (Upstate/Millipore) and incubated overnight at 4°C. β-catenin was measured using anti-β-catenin at 1:150 (BD Transduction Laboratories). c-Myc was stained using Abcam at 1:1000 (Y69). Phospho-S62 c-Myc (Abcam #51156) was used at 1:50 dilution and incubated overnight at 4°C.

Vectastain ABC Kit (Vector Laboratories) was used to perform all immunohistochemistry reactions. Dewaxing and antigen retrieval processing of sections was conducted as previously described[2].

For intratumoral c-Myc staining, high power fields were scored according to an index from 1-4 (a score of 1 denotes less than 25% of positive cells per high power field; a score of 2 denotes 25-50%; a score of 3 denotes 50-75%; a score of 4 denotes 75-100%). For intratmuoral phosphorylated S62 c-Myc, positive cells per tumor high power field were quantified according to an index from 1-5 (a score of 1 denotes less than 20% of positive cells per high power field; a score of 2 denotes 20-40%; a score of 3 denotes 40-60%; a score of 4 denotes 60-80; a score of 5 denotes 80-100%). Similarly, a β-catenin index was employed to quantify the extent of intratumoral nuclear and cytoplasmic staining. This index is generated by multiplying the staining intensity (on a scale of 100-500) by percentage of the cells demonstrating nuclear staining. For example, a score of 500 indicates a field that demonstrated very intense nuclear β-catenin stain while a score of 100 indicates a field that has weak nuclear β-catenin staining. Intratumoral proliferation was 7 by staining. Apoptosis and proliferation indices were generated by counting the number of positive cells per high-powered field (HPF; 40× objective) within each tumor by a blinded observer. In all tumor scoring, the average per mouse is presented and at least 5 power fields per animal were counted.

For RNA analysis, colonic tissue from mice was isolated and immediately placed into 350 µl RNALater (Qiagen) and stored at -80°C. RNA from tissue or cells was isolated

using the RNAEasy kit (Qiagen) according to the manufacturer's "Animal Tissue" protocol. RNA was subsequently stored at -80°C.

For RNA-seq experiments, RNA from WT colons (n=3), *Bves*$^{-/-}$ colons (n=3), WT tumors (n=3), and *Bves*$^{-/-}$ tumors (n=3) was sequenced by the Vanderbilt Technologies for Advanced Genomics (VANTAGE) core facility. Initial raw sequencing data were aligned to a reference mouse genome (mm9) using TopHat (version 1.3.1) software[3]. The transcript of mouse genome (mm9) was downloaded from UCSC as implemented in the Bioconductor package *GenomicFeatures*. Then the Bioconductor packages *Rsamtools* and *DESeq* were used to estimate the read count for expression of each gene and to detect differentially expressed (DE) genes. For count based gene expression data, *DESeq* uses a model based on the negative binomial distribution which includes a dispersion parameter to better estimate variance[4]. The p-values from *DESeq* were adjusted by Benjamini and Hochberg's method to control false discovery rate (FDR)[5].

BVES promoter methylation analysis

1) Primary Human Tissue Samples

Fresh frozen epithelial cell layers were isolated from each specimen using the epithelial "shake off" technique[6] and the DNA was extracted using Qiagen DNA extraction kits (Qiagen) following the manufacturer's instructions. DNA was extracted from the following groups: 1) 17 control samples of normal colon mucosa from patients who did not have UC (**Control-No UC**) 2) non-neoplastic cells from 11 UC patients without cancer/dysplasia (**Normal—no HGD/CAC**) 3) non-neoplastic cells from 10 UC patients with concurrent cancer/dysplasia located at least 20 cm away (**Normal—concurrent**

HGD/CAC) 4) cancerous or dysplastic cells from 10 UC patients (**HGD/CAC**). The specimens were obtained from the pathology archives at University of Washington (Seattle, WA) following protocols approved by the Institutional Review Board.

2) Methylation array analyses

300 ng of epithelial cell DNA was bisulfite converted using the EZ Meth DNA kit following the manufacturer's instructions (Zymo Research, #D5002). Converted DNA was applied to Infinium HumanMethylation450 BeadChips (Illumina) which were then processed in the Genomics Shared Resource Core at the Fred Hutchinson Cancer Research Center according to the manufacturer's specifications. Data was normalized and filtered as described by our group previously[7]. Differentially methylated loci (DML) were determined after converting beta values, which range from 0.0 (no methylation) to 1.0 (100% methylation), to M values, where the M value is the $\log_2$ ratio of the intensities of the methylated probe versus unmethylated probe. For the purposes of this study, we were interested in loci that demonstrated both 1) differential methylation between **UC—no HGD/CAC** and **UC—concurrent HGD/CAC** cases and 2) similar methylation patterns between **UC—concurrent HGD/CAC** and **HGD/CAC** cases. Loci with p values ≤ 0.0008 (adjusted p value ≤ 0.260) were considered differentially methylated.

The differentially methylated probes in the *BVES* promoter region were cg17398252 (located within a CpG island 1500 base pairs upstream from the transcription start site), cg25280433 (located within a CpG island in the 5' UTR/exon 1), and cg20624391 (located in a CpG island in 5' UTR/exon 1).

3) Pyrosequencing of DNA samples

Pyrosequencing assays were designed to confirm methylation differences seen on the HM450 arrays. Assays were designed to target the same promoter CpG island that contained the DML from the arrays. The same DNA samples that were used on the HM450 array were used for pyrosequencing, except for one UC—no HGD/CA and one UC—concurrent HGD/CAC case, both of which did not have enough DNA remaining for these assays. Primers and reaction conditions used have been previously described[8].

RNAScope

RNA scope was conducted according to manufacturer's protocol (ACD, www.acdbio.com) with probes directed against *BVES* (catalog number 410346), positive control Hs-PPIB (catalog number 313901), and negative control DapB (catalog number 310043Tissue microarrays were scanned digitally and uploaded to a digital image hub. The percentage of epithelium per core that stained positive was scored and quantified. Only cores that stained robustly with the positive control probe were scored. Clinical information of specimen is described in **Supplementary Table 2**.

Enteroid cultures

Enteroid cultures were derived according to previously published protocols[9]. Briefly, eight centimeters of small intestine were dissected, flushed with ice cold phosphate buffered saline (PBS), and opened lengthwise. Intestines were quickly rinsed, dissected into 5mm pieces, and washed in 5ml ice cold PBS for 15 minutes at 4^{o}C for 15 minutes. Fragments were then transferred to 5ml of chelation buffer (2mM EDTA, made fresh in

Dulbecco's PBS) and rocked for 30 minutes at 4°C. After removing chelation buffer, 5ml cold shaking buffer (PBS with 43.3mM sucrose and 54.9mM Sorbitol) was added and tissues were gently shaken for 4 minutes to free intestinal crypts. Resulting crypts were filtered through a 70µm filter, collected, and plated in Matrigel (Fisher Scientific, CB-40230C) at a concentration of 600 crypts per 50µl plug. After polymerization, Matrigel was overlaid with 500µl mini-gut media (Advanced DMEM/F12, B27, N2, Pen-strep, L-glutamine, HEPES) supplemented with 50 ng/ml EGF (R&D Systems, 2028-EG-200), 100 ng/ml Noggin (R&D Systems, 1967-NG-025/CF), 500 ng/ml R-Spondin (Vanderbilt Antibody and Protein Resource), and 200 ng/ml WNT3a (R&D Systems, 1324-WN-010). Growth media, containing all supplements with the exception of Wnt3a, was replaced every 4 days to maintain enteroid cultures.

Yeast two-hybrid assays

*BVES (*hgx2637v_pB29*)* and *PR61a* (pB20_A-197) constructs were obtained from Hybrigenics. Y2H assays were conducted as previously described[10].

Cell Culture

Unless otherwise indicated, all HEK 293T and Caco2 cells were cultured in DMEM with 10% serum and 1% Penn/strep. Polyethylenimine (PEI) at a concentration of 1 □g/ml was used for all transfection experiments. An empty vector was used to ensure equal quantities of cDNA were transfected. Cycloheximide (Sigma) was used at 100 □g/ml and cells were lysed at the indicated intervals. MG132 (CalBiochem) was used at 10 □M for 4 hours for ubiquitylation experiments.

BVES was knocked down using siRNA (Santa Cruz, 60295) or shRNA (Mission Sigma #143493), and *PR61α* was knocked down using an shRNA construct (Mission Sigma #10507). Scrambled siRNA (Santa Cruz 37007) or shRNA (Mission Sigma #SHC002) were used as controls.

Luciferase Reporter Assay

The E2F2 reporter was purchased from Switchgear genomics (ID:S720931).

The luciferase assays were conducted as previously reported using a SEAP plasmid as a transfection control[9]. Briefly, HEK 293T cells were plated in 6 well plates and each experimental condition as a technical triplicate.

Immunoprecipitation

For immunoprecipitation assays, cells were grown in 100-mm cell culture dishes. Once desired confluence was reached, cells were rinsed with ice-cold PBS and incubated for 15 min at 4°C in 1 ml of cell lysis buffer (Sigma) containing 1X Phosphatase inhibitor cocktail 2 and 3 (Sigma) and 1X Protease Inhibitor cocktail (Sigma). Samples were sonicated for 10 seconds at 4°C. Cellular debris was removed by centrifugation; protein concentration was measured by Bradford method. For immunoprecipitation, approximately 1 mg of total protein was incubated with 3 µg of the respective antibodies overnight at 4°C followed by a 3 hour incubation with 25 µl of protein A/G magnetic beads (Millipore). The immunoprecipitates were collected by magnetic separation and washed three times with 0.5 ml of cell lysis buffer. Washed beads were suspended in 50

μl of 2X Laemmli buffer and samples were resolved on a reducing 10% SDS-PAGE gel and probed with respective antibodies.

Proximity Ligation Assay

Proximity ligation assays (PLA) were performed according to manufacturer's protocol (Sigma, #DUO92101). Primary antibodies were incubated for 30 minutes in a 37°C humidified chamber at 0.250 ug/ul. HA (Invitrogen), V5 (Abcam), c-Myc (cell signaling), PPP2R5A (Bethyl labs), BVES (Abcam).

Western Blots

For western blots, cells were washed with ice-cold PBS before being scraped and collected. Cells were pelleted by centrifugation and resuspended in 2X Laemmli buffer and boiled for 10 minutes before analysis by SDS-PAGE electrophoresis. Membranes were blocked using Odyssey blocking buffer for 30 minutes and then blotted with anti-PPP2R5A (Bethyl labs, #A300-967A), anti-c-Myc (Cell Signaling #D84C12), anti-V5 (Abcam #ab27671), anti-His (Abcam #ab18184), or anti-HA (Vanderbilt Antibody and Protein Resource). All antibodies were used at 1:1000 concentration in Odyssey blocking buffer with 0.1% Tween-20. Primary antibodies were incubated for 1 hour at room temperature (RT) before being washed three times in PBS-Tween. LiCor secondary antibodies were used at 1:30,000 dilution and incubated for 30 minutes at room temperature. Quantification of western blot band intensity was conducted using LiCor Image Studio.

Plasmids

BVES and PR61α expression plasmids were generated using Gateway cloning (Invitrogen). pENTR vectors containing either BVES (HsCD00368575, Harvard Plasmid Prep) or PPP2R5A (HsCD00041318, Harvard Plasmid Prep) were shuttled into pcDNA3.1 V5/His using LR clonase (Invitrogen). The HA-tagged PP2Ac expression plasmid was graciously provided by Peter Howley who deposited the plasmid into Addgene repository (plasmid #35005). WT-c-Myc and T58A-c-Myc plasmids were previously described[12].

qPCR

For quantitative reverse transcription polymerase chain reactions, twenty microliters of cDNA was synthesized using iScript cDNA Synthesis Kit (Bio-Rad) from 1 μg of RNA per sample. All RT-PCR reactions were carried out using SYBR green reaction mix (Bio-Rad) according to the manufacturer's protocol.

The following primers were used to measure expression levels: human *CAD*: (F: AGTGGTGTTTCAAACCGGCAT and R:CAGAGGATAGGTGAGCACTAAGA), human *ODC* (F:TTTACTGCCAAGGACATTCTGG and R: GGAGAGCTTTTAACCACCTCAG) and mouse *Odc* (F: AGCAGGCTTCTCTTGGAAC and R: CATGCATTTCAGGCAGGTTA). All qPCR reactions were normalized to GAPDH (Human GAPDH, Realtime Primers #3541 and Mouse Gapdh, Realtime Primers #7317).

Statistical Methods

Throughout the paper, if more than two groups were being analyzed, a one-way ANOVA with New Keuls post-hoc test was used. If only two groups were being compared, a Student's *t* test was used. In all analyses using IHC, the observer was blinded to slide identity, and the slide was scored in an unbiased fashion.

REFERENCES

1. Andrée B, Fleige A, Arnold HH, et al. Mouse Pop1 is required for muscle regeneration in adult skeletal muscle. Mol Cell Biol 2002;22(5):1504–1512.
2. Barrett CW, Fingleton B, Williams A, et al. MTGR1 is required for tumorigenesis in the murine AOM/DSS colitis-associated carcinoma model. Cancer Res 2011;71(4):1302–1312.
3. Trapnell C, Pachter L, and Salzberg SL. TopHat: discovering splice junctions with RNA-Seq. Bioinformatics 2009;25(9): 1105-1111.
4. Anders S, and Huber, W. Differential expression analysis for sequence count data. Genome Biology 2010;11(10): R106.
5. Benjamini Y, Drai D, Elmer G, et al. Controlling the false discovery rate in behavior genetics research. Behav Brain Res 2001; 125 (1-2): 279-284.
6. Risques RA, Lai LA, Brentnall TA, et al. Ulcerative colitis is a disease of accelerated colon aging: evidence from attrition and DNA damage. Gastroenterology 2008;135 (2): 410–418.
7. Luo, Y, Wong CJ, Kaz AM, et al. Differences in DNA methylation signatures reveal multiple pathways of progression from adenoma to colorectal cancer. Gastroenterology 2014;147 (2): 418–429.
8. Williams CS, Zhang B, Smith JJ, et al. BVES regulates EMT in human corneal and colon cancer cells and is silenced via promoter methylation in human colorectal carcinoma. J Clin Invest 2011;121(10):4056–4069.
9. Parang B, Rosenblatt D, Williams AD, et al. The transcriptional corepressor MTGR1 regulates intestinal secretory lineage allocation. FASEB J 2014;29(3):786–795.

10. Barrett CW, Smith JJ, Lu LC, et al. Kaiso directs the transcriptional corepressor MTG16 to the kaiso binding site in target promoters. PLoS One 2012;7(12):e51205.
11. Salghetti SE, Kim SY, Tansey WP. Destruction of Myc by ubiquitin-mediated proteolysis: Cancer-associated and transforming mutations stabilize Myc. EMBO J 1999;18(3):717-726

Supplementary Figures 1-8 and Supplementary Tables 1-2

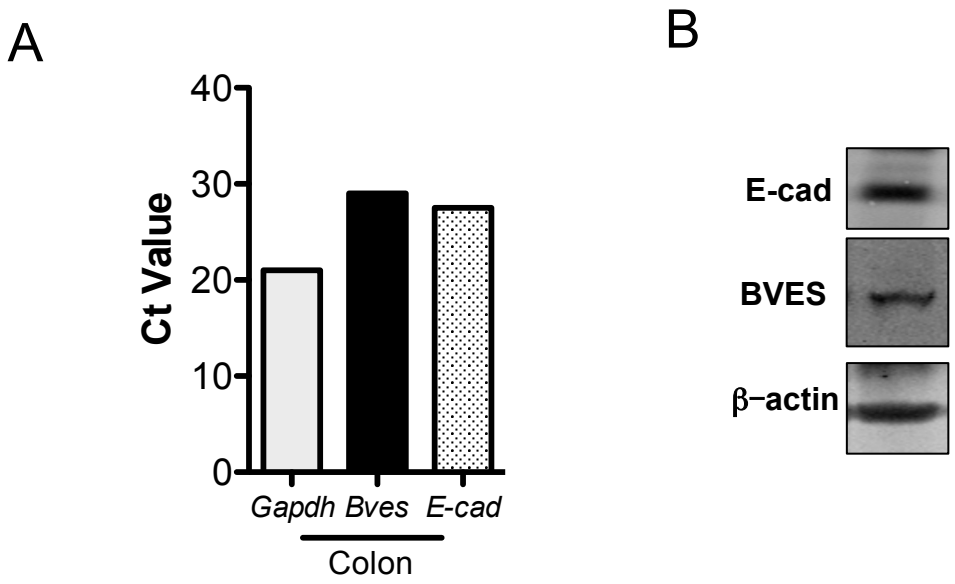

Supplementary Figure 1 A) *Ct* values of *Gapdh, Bves,* and *E-cadherin* mRNA levels in WT mouse colons. **B)** Immunoblot of E-cadherin, BVES and β-actin in mouse colons.

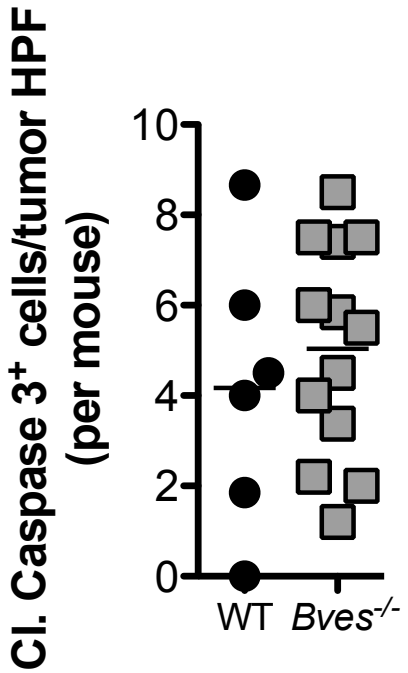

Supplementary Figure 2
Quantification of cleaved caspase 3 positive cells per tumor high-powered field.

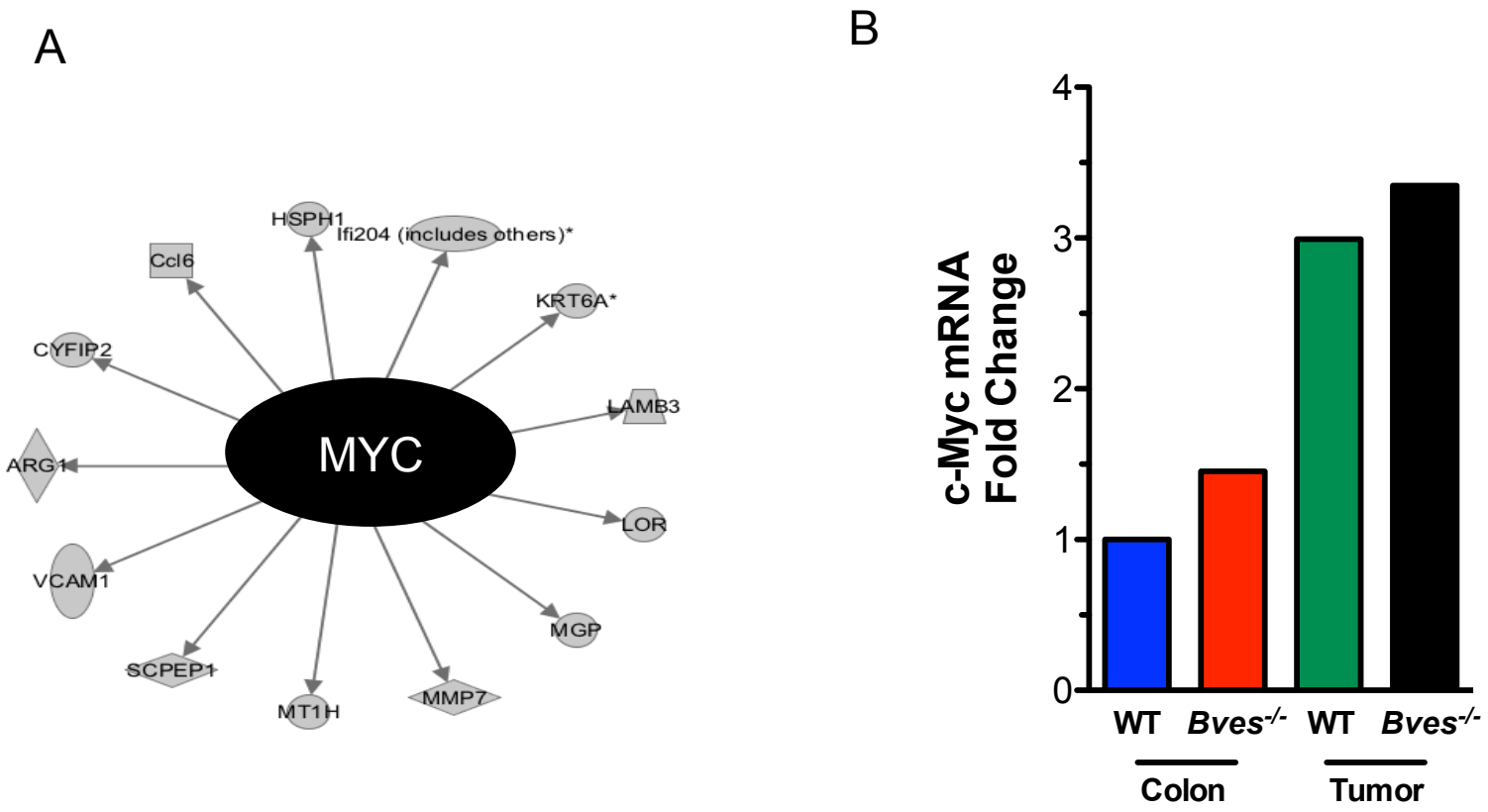

Supplementary Figure 3

(A) IPA generated schematic of dysregulated c-Myc network in *Bves*$^{-/-}$ tumors compared to WT tumors. (**B)** c-Myc mRNA levels relative to WT colon.

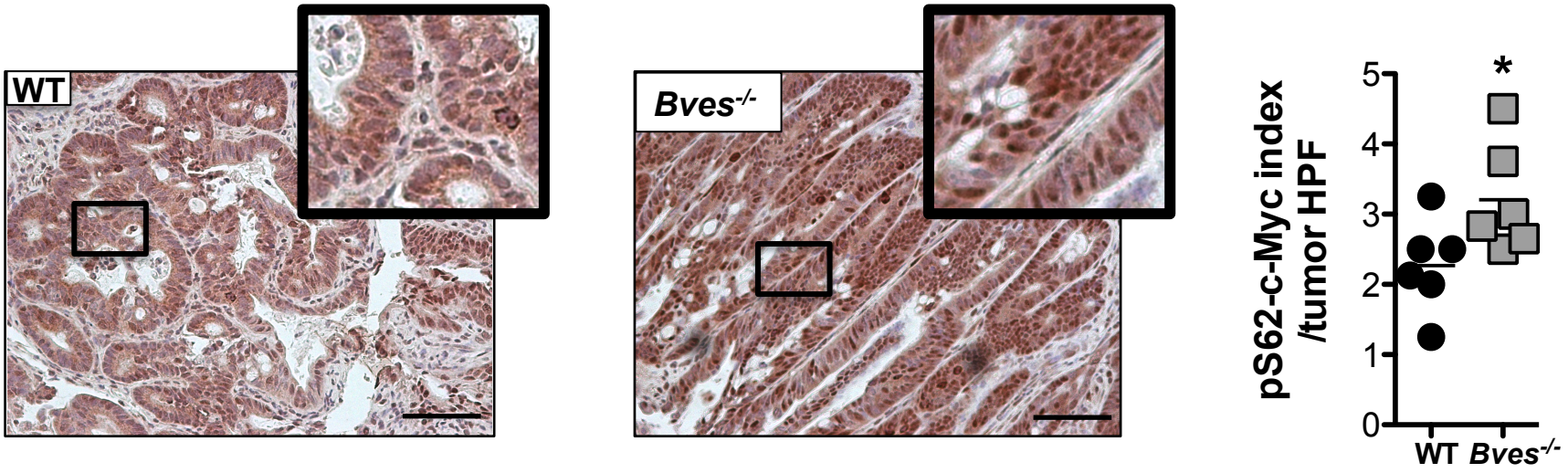

Supplementary Figure 4

Left: Representative images of immunohistochemistry for intratumoral phosphorylated serine 62 c-Myc staining. Right: Quantification of pS62 c-Myc positive cells per tumor high power field. High power fields were scored according to an index from 1-5 (a score of 1 denotes less than 20% of positive cells per high power field; a score of 2 denotes 20-40%; a score of 3 denotes 40-60%; a score of 4 denotes 60-80; a score of 5 denotes 80-100%). Each dot represents the average score of each mouse per tumor HPF. A minimum of 5 HPF were scored per mouse. Student's t test, *p<0.05. Size standard=50 microns.

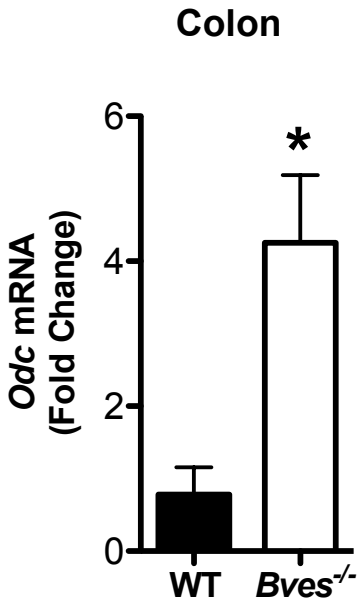

Supplementary Figure 5

qPCR for c-Myc transcriptional target *Odc* in colons of WT and *Bves*$^{-/-}$ mice at baseline. *p<0.05

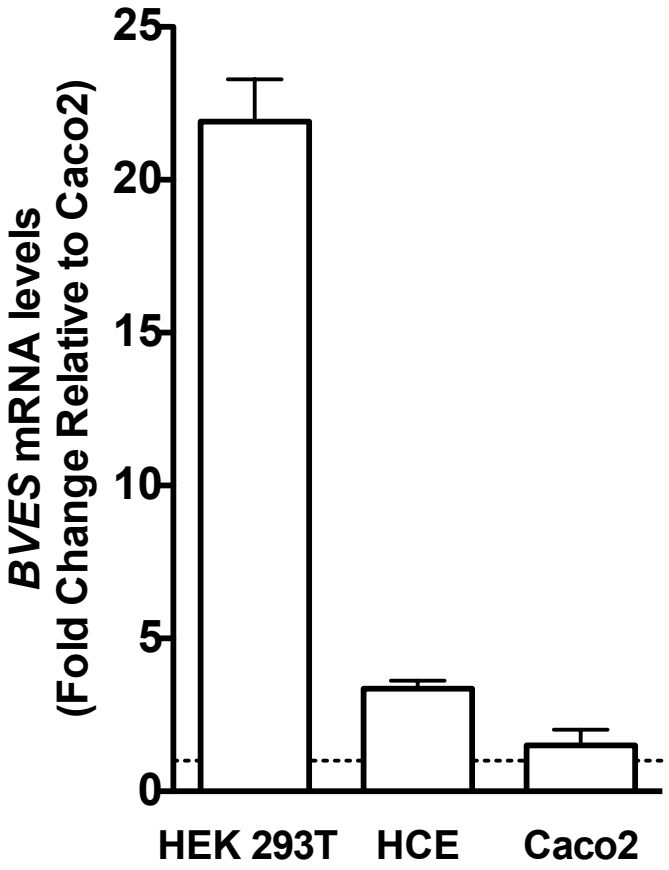

Supplementary Figure 6
qPCR of *BVES* mRNA in three human cell lines: HEK 293T, Human Corneal Epithelial (HCE), and Caco2.

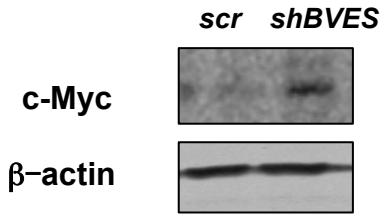

Supplementary Figure 7
Immunoblot of c-Myc after knockdown of *BVES* in the Human Corneal Epithelial (HCE) cell line using shRNAs.

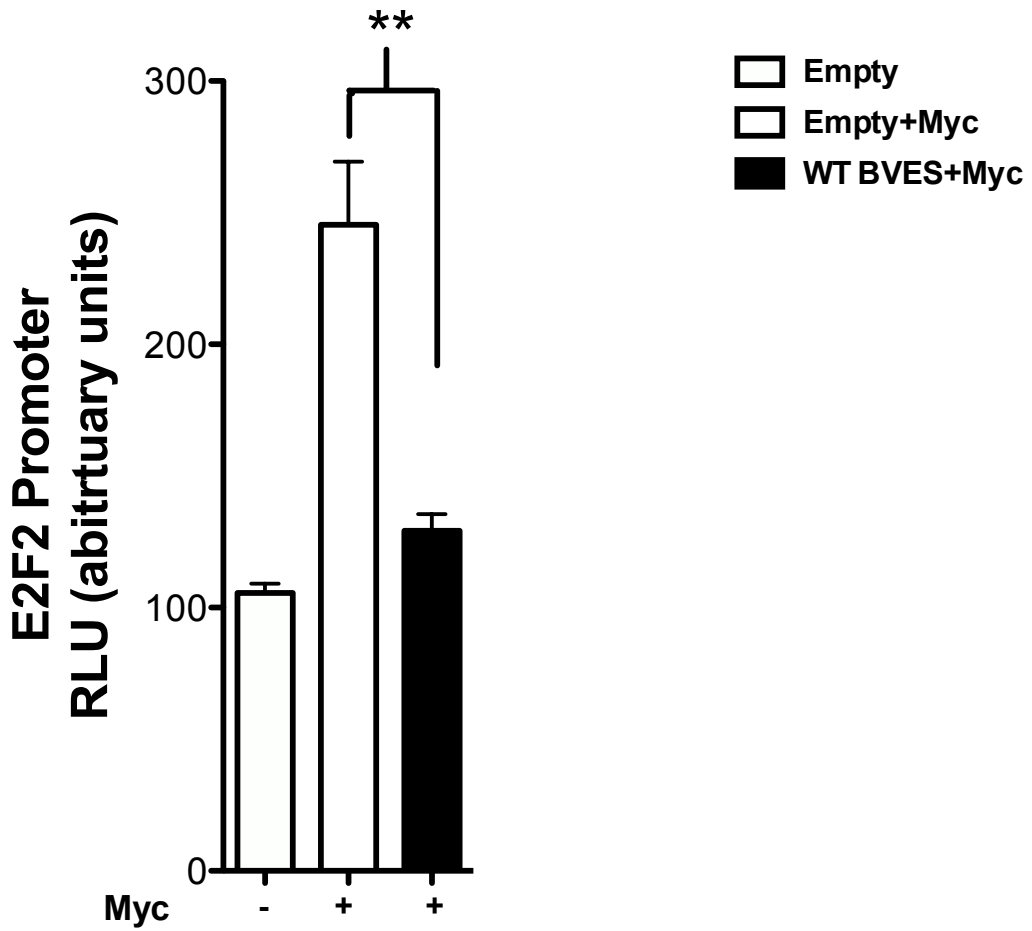

Supplementary Figure 8

Relative luciferase values of HEK 293T cells co-transfected with an E2F2 reporter and an empty vector, HA-c-Myc and/or V5-BVES. Experiment was performed in technical triplicates and replicated twice. **p<0.01

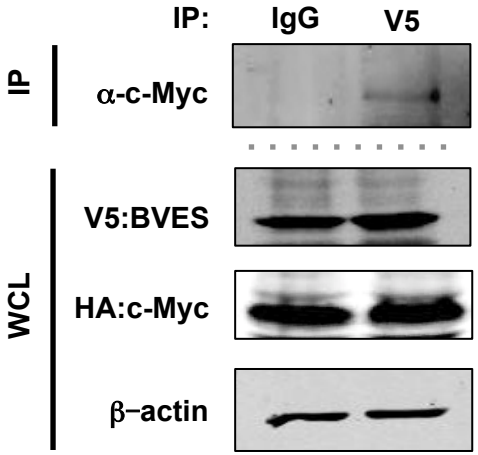

Supplementary Figure 9

HEK 293T cells were transfected with HA:c-Myc and V5:BVES. V5:BVES was immunoprecipitated followed by immunoblotting for HA:c-Myc. Non-specific IgG was used as a control.

Supplementary Table 1

Patient	Biopsy dx	UC NP/P	biopsy dx	Location	Distance to Dysplasia(f/ anal verge)	Age	Gender	Disease Duration(mo.)	PSC?	Disease Activity	Inflammation
1	neg	NP	neg	distal		67	M	30	no		3-4+
2	neg	NP	neg	distal		70	F	16	no		3-4+
3	tumor	P	tumor	distal	0 cm	55	F	20	no		4+
4	neg	NP	neg	distal		56	F	10	no		
5	tumor	P	tumor	proximal	0 cm	47	M	8	no		?
6	tumor	P	tumor	proximal	0 cm	31	M	10	no		?
7	neg	NP	neg	distal		48	M	9	no		3-4+
8	neg	P	neg	distal		67	M	30	no		0
9	neg	NP	neg	distal		41	F	20	no		2-3+
10	neg	NP	neg	distal		63	M	39	no		
11	neg	NP	neg	distal		31	M	8	no		3-4+
12	neg	NP	neg	distal		49	F	20	no		1-2+
13	HGD	P	HGD	83 cm	0 cm	36	M	8	yes	marked activity	4+
14	HGD	P	HGD	(C2)next to rectal pieces	0 cm	53	F	NA	no?		4+
15	neg	NP	neg	7 cm		59	M	0.25		no data	active
16	neg	NP	neg	14 cm		51	F	20	no	no data	3+
17	neg	NP	neg	15 cm		46	F	17	no	no data	0
18	neg	P	neg	3.4 cm	78.3 cm	36	M	11	yes	no data	0
19	HGD	P	HGD	92 cm	0 cm	58	M	29	yes	focal activity	0
20	HGD	P	HGD	3 cm	0 cm	32	M	16	no	active	1+
21	HGD	P	LGD +HGD	19 cm	0 cm	48	M	10	no	focal activity	0
22	HGD	P	HGD	4 cm	0 cm	33	M	13	no	focal active	4+
23	HGD	P	HGD	70.4 cm	6.4cm to CA	51	F	13	yes	active	1+
24	HGD	P	HGD	31.2 cm	0 cm	33	F	22	no	no data	1+
25	neg	P	neg	14.4 cm	18.4 cm	34	M	17	yes	active	1+

Supplementary Table 2

	UC Patients With Cancer (N=14)	UC Patients with Dysplasia (N=5)	UC patients (N=13)	Normal (N=11)
Average Age (sd)	51.4 ± 18.3	53.2 ± 15.5	55± 10.2	60.9 ± 11.5
Gender	6 Males, 8 Females	4 Males, 1 Female	8 Males, 5 Females	5 Males, 6 Females
BMI	26 ± 9.2	n/a	n/a	26.6 ± 3.1
Race	White (N=14)	n/a	n/a	Black (N=1), White (N=10)
Tumor Grade	Grade 1 (N=3), Grade 2 (N=2), Grade 3 (N=9)	n/a	n/a	n/a
Location if known	Descending (N=2), Transverse (N=2), Left (N=1), Ascending (N=1), Sigmoid (N=2), Rectum (N=4), Hepatic fixture (N=1)	n/a	n/a	n/a
Lymph Node Involvement	Positive (N=9), Negative (N=5)	n/a	n/a	n/a
Average Tumor Size	4.2 ± 2.9 cm	n/a	n/a	n/a
Mesenteric Deposits	Absent (N=7), Present (N=8)	n/a	n/a	n/a

BVES regulates c-Myc stability via PP2A and suppresses colitis-induced tumorigenesis

Short Title: BVES suppresses inflammatory carcinogenesis

Bobak Parang[1,2], Andrew M. Kaz[3,4], Caitlyn W. Barrett[1,2], Sarah P. Short[1,2], Wei Ning[1,2], Cody E. Keating[1,2], Mukul K. Mittal[1,2], Rishi D. Naik[1], Mary K. Washington[5], Frank L. Revetta[5], J. Joshua Smith[6], Xi Chen[8], Keith T. Wilson[1,2,8,9], Thomas Brand[10], David M. Bader[11], William P. Tansey[8,11], Ru Chen[4], Teresa A. Brentnall[4], William M. Grady[4,12], Christopher S. Williams[1,2,8,9]

[1]Department of Medicine, Division of Gastroenterology, Vanderbilt University; [2]Department of Cancer Biology, Vanderbilt University; [3]Research and Development Service, VA Puget Sound Health Care System; [4]Department of Medicine, Division of Gastroenterology, University of Washington, Seattle; [5]Department of Pathology, Microbiology, and Immunology, Vanderbilt University; [6]Department of Surgery, Vanderbilt University; [7]Department of Biostatistics, Vanderbilt University; [8]Vanderbilt Ingram Cancer Center; [9]Veterans Affairs Tennessee Valley Health Care System, Nashville, TN; [10]Department of Developmental Dynamics, Imperial College of London; [11]Department of Cell and Developmental Biology, Vanderbilt University; [12]Clinical Research Division, Fred Hutchinson Cancer Research Center

Keywords: Cancer, IBD, Ulcerative colitis, Colonic neoplasms, Colorectal cancer

Corresponding Author:
Christopher S. Williams, M.D., Ph.D.
Associate Professor of Medicine and Cancer Biology
Director, Physician Scientist Training Program
Staff Physician, VA Health System
Vanderbilt University School of Medicine
1065D MRB-IV
B2215 Garland Ave
Nashville, TN 37232

Disclosure of Potential Conflicts of Interest: The authors have no conflicts of interest to disclose.

Author Contributions: BP and **AMK** contributed equally to the work in the manuscript. **WMG** and **CSW** are co-corresponding authors. BP, AMK, CWB, and SPS developed the hypothesis, designed experiments, analyzed the data, and wrote the manuscript. BP, AMK, CWB, SPS, CEK, WN, MKM, RDN, FLR performed experiments. BP, AMK, CWB, SPS, MKW, JJS, XC, KTW, TAB, DMB, WPT, RC, TAB, WMG, CSW contributed to experimental design, generation of the reagents, and manuscript editing. BP, AMK, WMG, CSW conceived and supervised the project.

Word Count: 3788

ABSTRACT:

Objective: *Blood vessel epicardial substance* (BVES) is a tight junction-associated protein that regulates epithelial-mesenchymal states and is underexpressed in epithelial malignancy. However, the functional impact of BVES loss on tumorigenesis is unknown. Here we define the *in vivo* role of BVES in colitis-associated cancer (CAC), its cellular function, and its relevance to inflammatory bowel disease (IBD) patients.

Design: We determined *BVES* promoter methylation status using an Infinium HumanMethylation450 array screen of patients with ulcerative colitis with and without CAC. We also measured *BVES* mRNA levels in a tissue microarray consisting of normal colons and CAC samples. *Bves*$^{-/-}$ and wild-type mice (controls) were administered azoxymethane (AOM) and dextran sodium sulfate (DSS) to induce tumor formation. Lastly, we utilized a yeast two-hybrid screen to identify BVES interactors and performed mechanistic studies in multiple cell lines to define how BVES reduces c-Myc levels.

Results: *BVES* mRNA was reduced in tumors from patients with CAC via promoter hypermethylation. Importantly, *BVES* promoter hypermethylation was concurrently present in distant non-malignant appearing mucosa. As seen in human patients, *Bves* was underexpressed in experimental inflammatory carcinogenesis, and *Bves*$^{-/-}$ mice had increased tumor multiplicity and degree of dysplasia after AOM/DSS administration. Molecular analysis of *Bves*$^{-/-}$ tumors revealed Wnt activation and increased c-Myc levels. Mechanistically, we identified a new signaling pathway whereby BVES interacts with PR61α, a PP2A regulatory subunit, to mediate c-Myc destruction.

Conclusions: Loss of BVES promotes inflammatory tumorigenesis through dysregulation of Wnt signaling and the oncogene c-Myc. *BVES* promoter methylation status may serve as a CAC biomarker.

SUMMARY BOX

What is already known about this subject?

- Patients with ulcerative colitis are at greater risk for developing colon cancer.
- Blood vessel epicardial substance (BVES) is a tight junction protein that regulates epithelial-to-mesenchymal transition *in vitro*.
- c-Myc is an oncogene overexpressed in 50% of all malignancies, including colitis-associated cancer (CAC).
- **What are the new findings?**
- *BVES* promoter hypermethylation is present in CAC and distant uninvolved mucosa.
- *BVES* is underexpressed in patients with CAC compared to normal colonic tissue.
- Deletion of *Bves* promotes colitis-associated tumor multiplicity and dysplasia.
- BVES directs the PR61α-PP2A complex to target c-Myc for proteasomal destruction.

How might it impact on clinical practice in the foreseeable future?

- *BVES* promoter hypermethylation status is a potential biomarker to identify UC patients at risk for cancer.
- Our studies demonstrate a new mechanism for regulation of c-Myc, an oncogene that is dysregulated in numerous malignancies.
- BVES plays a key role in maintaining the integrity of the colonic mucosa and protecting from inflammatory carcinogenesis, and may represent a therapeutic target in CAC.

INTRODUCTION

Chronic inflammation promotes the development of colorectal cancer **(CRC)**[1,2]. Patients with inflammatory bowel disease (**IBD**), for example, have an elevated risk of developing CRC[3], particularly those who have extensive disease or long disease duration[4]. Although the pathogenesis of inflammatory carcinogenesis remains unclear, at least one component of malignant degeneration is thought to be disruption of intestinal epithelial function as a consequence of chronic inflammation[5,6]. Indeed, pathologic changes in adherens and tight junction proteins have been described in colitis and colitis-associated cancer (**CAC**)[6–8]. In addition to providing junctional integrity between cells, adherens and tight junctional complexes also transduce extracellular signals to direct intracellular programs ("outside-in" signaling[9]), such as those controlling cellular proliferation and differentiation. For example, E-cadherin can sequester β-catenin at the cell membrane, preventing its nuclear localization and transcriptional activity[10]. Given that dysregulation of junctional proteins commonly occurs in CAC, understanding their function in normal biology may yield clues to how their dysfunction promotes carcinogenesis.

Blood vessel epicardial substance (**BVES/POPDC1**) is a tight junction-associated protein often silenced in carcinomas secondary to promoter hypermethylation[11–13]. Restoring *BVES* expression in CRC cell lines promotes epithelial-like morphology and decreases proliferation, migration, invasion, xenograft tumor growth, and metastasis, together indicating broad regulatory capabilities[11]. Conversely, knockdown of *BVES* in epithelial-like cells induces a mesenchymal-like phenotype characterized by increased proliferation, altered morphology, and disorganized cell-cell contacts[11]. Yet how BVES

regulates these phenotypes is incompletely understood. Indeed, while several BVES interacting proteins have been identified[11], their known functions do not explain fully the role of BVES in maintaining epithelial phenotypes. Moreover, how BVES contributes to tumor development has not been tested using genetic approaches.

The transcription factor c-Myc is commonly overexpressed in cancer[14,15] and regulates proliferation, differentiation, apoptosis, and epithelial-to-mesenchymal transition[16]. In mouse models of sporadic CRC, decreased c-Myc levels reduce *Apc*-driven tumorigenesis[17]. In IBD, c-Myc is overexpressed in both inflamed tissues and CAC tumors[18], and network analysis of CAC samples indicated that c-Myc dysregulation functionally contributes to CAC progression[19]. c-Myc levels are also increased in experimental models of inflammatory carcinogenesis, such as the azoxymethane (**AOM**)/dextran sodium sulfate (**DSS**) mouse model of CAC[20]. Yet the processes responsible for c-Myc dysregulation in inflammatory carcinogenesis remain unidentified. To date, a complex network of proteins—including protein phosphatase 2A (PP2A), Axin1, and GSK3β—has been identified that regulates c-Myc protein levels by modifying the phosphorylation status of c-Myc at two residues, threonine 58 (**T58**) and serine 62 (**S62**)[21]. Ubiquitylation of c-Myc is initiated by phosphorylation at T58, leading to its ultimate degradation. Given the prominent role of c-Myc in driving oncogenic programs, understanding mechanisms that control PP2A dephosphorylation of c-Myc may identify new therapeutic targets in inflammatory carcinogenesis.

Here we report that BVES is an important regulator of inflammatory carcinogenesis programs and promotes c-Myc degradation through an interaction with the PR61α-PP2A complex. We observed that *BVES* is reduced in human CAC samples, and

further that the *BVES* promoter was hypermethylated within the tumors and at distant unaffected mucosa, suggesting a field effect. Using the AOM/DSS inflammatory carcinogenesis model, we determined that *Bves*$^{-/-}$ mice demonstrate greater tumor incidence and multiplicity as well as a higher degree of dysplasia and intratumoral proliferation. Furthermore, molecular analysis of *Bves*$^{-/-}$ tumors revealed increased c-Myc protein and signaling activity. c-Myc protein was also elevated in intestinal crypts from *Bves*$^{-/-}$ mice. In line with *in vivo* results, knockdown of BVES *in vitro* increased c-Myc stability and consequently increased expression of key c-Myc targets *ODC* and *CAD*. Conversely, BVES overexpression reduced c-Myc stability and increased c-Myc ubiquitylation. Using a yeast two-hybrid (**Y2H**) screen, we identified PR61α, the PP2A regulatory subunit critical for c-Myc degradation, as a BVES-interacting protein, and show that this interaction is required for BVES to modulate cellular c-Myc levels. Thus, we demonstrate that BVES coordinates PR61α-containing PP2A phosphatase complexes to restrict c-Myc protein levels and that BVES is a key suppressor of inflammatory carcinogenesis whose promoter methylation status may define patients with ulcerative colitis (**UC**) at risk for colon cancer.

MATERIALS AND METHODS

Mice, treatments, and analysis

AOM and DSS were prepared as previously described[22]. *Bves*$^{-/-}$ mice have been previously described[23]. Detailed protocols can be found in the **Supplementary Materials and Methods Section**.

BVES promoter methylation analysis

Tissue samples were obtained from colectomy specimens from individuals without UC, individuals with UC but without dysplasia or cancer, and UC patients with high-grade dysplasia and/or colon cancer. Clinical information is described in online **supplementary table 1.** Detailed protocols regarding epithelial isolation, methylation array, and pyrosequencing can be found in the **Supplementary Materials and Methods Section.**

See **Supplementary Materials and Methods** for detailed methods regarding cell culture experiments, RNA scope, promoter methylation analyses, and mouse analysis.

RESULTS

BVES is downregulated and its promoter is hypermethylated in CAC

As *BVES* is underexpressed via promoter hypermethylation in CRC[11], we asked whether the *BVES* promoter was also hypermethylated in CAC. Therefore, we analyzed *BVES* methylation status in an Infinium HumanMethylation450 array screen of IBD samples. The samples consisted of control patients (**Control—No UC**), patients with UC who did not have cancer (**UC—no HGD/CAC**), and two different types of samples from patients with UC who had colon cancer: the remote, non-malignant tissue (**UC—concurrent HGD/CAC**) and tissue with high-grade dysplasia and/or cancer (**HGD/CAC**). These analyses demonstrated that the *BVES* promoter was unmethylated in the controls–No UC (0.1% ± 0.016%), moderately methylated in UC–no HGD/CAC (16% ± 4.7%), and hypermethylated in the HGD/CAC among patients with colitis-associated carcinoma (HGD/CAC, 53% ± 2.6%) (**figure 1A**). Furthermore, remote non-neoplastic, mucosal samples (UC-Concurrent HGD/CAC) from the same patients who had CAC (HGD/CAC) were hypermethylated (50% ± 2.6%) to a similar degree as that observed in cancerous tissue. Interestingly, these results suggest that *BVES* promoter methylation may represent a field effect in CAC and that *BVES* promoter methylation status may identify UC patients with concurrent malignancy. To confirm the results derived from the HM450 methylation array studies, we pyrosequenced the *BVES* promoter in the same samples and again demonstrated low levels of methylation in the UC—no HGD/CAC cases, and higher methylation in both the UC—concurrent HGD/CAC and HGD/CAC cases (**figure 1B**).

It is possible that *BVES* promoter methylation, while increased, may not be sufficient to silence its expression. To determine whether *BVES* promoter methylation indeed reduced its transcription, we tested whether *BVES* mRNA was downregulated in CAC using high resolution *in situ* hybridization (RNAScope[24]) in a tissue microarray consisting of normal, UC, and CAC samples. *BVES* mRNA levels were low, but consistently present in normal colonic epithelial cells (**figure 1C**). In UC and CAC samples, however, *BVES* message was rarely detected and quantification of epithelial staining indicated a 5-fold decrease ($p<0.001$). Taken together, *BVES* RNA expression is downregulated in both UC and CAC, most likely due to promoter hypermethylation. Furthermore, as the *BVES* promoter is hypermethylated in both tumor and non-malignant mucosa in patients with CAC, *BVES* promoter methylation may serve as a biomarker associated with dysplasia or neoplasia in patients with IBD.

Bves loss promotes CAC development

While *BVES* underexpression was consistently observed in human CAC, these studies do not establish whether BVES loss actively promotes tumorigenesis. Therefore, we used mouse genetic approaches combined with the AOM/DSS model (**figure 2A**) to determine if BVES loss contributed to inflammatory tumorigenesis. While *Bves* was expressed at baseline in the murine colon at both the RNA and protein levels (see online **supplementary figure 1**), transcriptome profiling of AOM/DSS-induced tumors in WT mice showed a 5-fold decrease in *Bves* transcripts (**figure 2B**), mirroring the results observed in human CAC. As expected**,** we also observed changes in other tight junction constituents, supporting previous reports of tight junctional dysregulation in colitis and CAC[25]. We confirmed that *Bves* message was decreased in AOM/DSS tumor tissue by

qPCR in an independent sample set (**figure 2B**). Interestingly, *Bves* message also decreased in AOM/DSS treated non-malignant tissue compared to normal colons (**figure 2B**), again suggesting a field effect in inflammatory carcinogenesis. As a result, we hypothesized that complete loss of *Bves* might promote inflammatory carcinogenesis.

To test the effect of *Bves* loss in CAC, we compared WT and *Bves*$^{-/-}$ mice subjected to the same inflammatory carcinogenesis protocol. We first observed that *Bves*$^{-/-}$ mice lost a greater fraction of body weight compared to WT mice, most notably during cycle 3 (**figure 2C**), suggesting increased sensitivity to AOM/DSS treatment. Indeed, endoscopy one-week prior to sacrifice demonstrated increased tumor multiplicity in *Bves*$^{-/-}$ mice (**figure 2D)** and this was confirmed at necropsy where we observed 100% tumor penetrance in *Bves*$^{-/-}$ mice compared to 60% in WT mice (**figure 2E**). *Bves*$^{-/-}$ mice also demonstrated increased tumor multiplicity (6.5 ± 0.6 tumors per *Bves*$^{-/-}$ mouse vs. 2.2± 0.5 tumors per WT mouse, $p<0.001$), and tumor size (**figure 2E**). Furthermore, *Bves*$^{-/-}$ tumors exhibit more advanced dysplasia compared to WT tumors (**figure 2F**). Control mice treated with three cycles of DSS-only or a single AOM injection did not develop tumors during this time-frame (data not shown). Taken together, these results suggest that BVES underexpression in CAC functionally contributes to inflammatory carcinogenesis.

Increased proliferation and enhanced Wnt activation in *Bves*$^{-/-}$ tumors

To identify BVES-directed mechanisms responsible for modifying tumorigenesis, we examined proliferation and apoptosis in the tumors of AOM/DSS treated *Bves*$^{-/-}$ mice. Proliferation, as measured by phospho-histone H3 staining, was increased in *Bves*$^{-/-}$ tumors (**figure 3A)**. Conversely, staining for cleaved caspase-3 indicated no difference in intratumoral apoptosis between *Bves*$^{-/-}$ and WT mice (**see online supplementary figure**

2). As Wnt activation can drive proliferation, we postulated that Wnt signaling might be perturbed in *Bves*$^{-/-}$ tumors. β-catenin dysregulation is a key indicator of hyperactive Wnt signaling[26], and β-catenin is also a mutational target in DMH/DSS inflammatory carcinogenesis, resulting in increased levels and altered subcellular distribution[27]. Therefore, we analyzed β-catenin by immunohistochemistry and observed excessive cytoplasmic and nuclear β-catenin localization in *Bves*$^{-/-}$ tumors compared to WT tumors (**figure 3B**). While these results suggested hyperactive Wnt signaling in *Bves*$^{-/-}$ tumors, we confirmed this by RNA-seq analysis, which indicated upregulation of established Wnt targets, such as *Mmp7, Wisp2,* and *Rspo4* (**figure 3C**), in *Bves*$^{-/-}$ tumors. Ingenuity Pathway Analysis (**IPA**)[28] of the RNA-seq data set also indicated hyperactive Wnt networks, such as *β-catenin* and *Tcf*. Finally, immunoblotting demonstrated greater expression of cyclin D1 and c-jun, two well-characterized Wnt target genes[29,30], in *Bves*$^{-/-}$ tumors (**figure 3D**). While previous experiments demonstrated that BVES could regulate Wnt signaling using *in vitro*, cell-based assays[11], these findings provide the first *in vivo* and genetic evidence supporting the hypothesis that BVES regulates Wnt activity.

BVES regulates c-Myc degradation

As c-Myc is a *bona-fide* Wnt transcriptional target[17], has been identified as a potential biomarker in patients with IBD at risk for CAC[19], and is overexpressed in AOM/DSS tumors[20], we postulated that c-Myc was dysregulated in *Bves*$^{-/-}$ tumors. Indeed, IPA analysis of intratumoral transcriptomes identified causal dysregulation[28] of c-Myc networks (**see online supplementary figure 3A**). While analysis of RNA-seq datasets showed only a modest increase in c-Myc transcripts in *Bves*$^{-/-}$ tumors compared to WT tumors (see online **supplementary figure 3B**), immunohistochemical staining for

c-Myc demonstrated an increase in both total c-Myc protein (**figure 4A**) and transcriptionally active, phosphorylated serine 62 c-Myc species in *Bves*$^{-/-}$ tumors (see online **supplementary figure 4**). Interestingly, immunoblotting in tumor-adjacent mucosa also showed higher c-Myc levels in *Bves*$^{-/-}$ colons, which suggested c-Myc was increased prior to tumor formation and that BVES might regulate c-Myc levels in the gut at baseline (**figure 4B**). To test this, we isolated crypts from untreated *Bves*$^{-/-}$ and WT mice and observed greater c-Myc protein in *Bves*$^{-/-}$ samples (**figure 4C**). Consistent with elevated c-Myc, qPCR for *Ornithine decarboxylase (Odc)*, a c-Myc transcriptional target, indicated a 4-fold increase in *Bves*$^{-/-}$ colons (see online **supplementary figure 5**). We also observed increased mRNA of c-Myc targets *Odc* and *E2f transcription factor 2 (E2f2)* (**figure 4D**) in "mini-gut" 3D cultures, demonstrating that BVES regulation of c-Myc activity was epithelial cell-autonomous.

As we observed increased c-Myc protein in *Bves*$^{-/-}$ tumors, we postulated that BVES could regulate c-Myc protein stability. Three cell lines—HEK 293T (non-malignant cell line), Caco2 (CRC cell line that can form a polarized epithelium), and HCE (Human Corneal Epithelial)—which all express BVES **(supplementary figure 6)**[11] were used for BVES knockdown experiments. In all three cell lines, *BVES* RNAi increased c-Myc protein levels (**figure 5A and supplementary figure 7**). In addition to increasing total c-Myc protein, we also observed that *BVES* knockdown reduced T58 phosphorylation, a key post-translational modification which signals for c-Myc degradation by the ubiquitin-proteasome system (**figure 5A**). This increase in c-Myc was functionally relevant as transcript levels of c-Myc targets *ODC* and *Carbamoyl-Phosphate Synthetase 2 Aspartate Transcarbamylase and Dihydroorotase* (*CAD*) were

increased with *BVES* knockdown (**figure 5B**). Furthermore, knockdown of BVES doubled c-Myc half-life compared to non-targeting control samples (**figure 5C**). Conversely, overexpressing BVES reduced c-Myc protein levels, increased T58 c-Myc species (**figure 5D**), dampened c-Myc transcriptional activation of the c-Myc responsive E2F2 reporter (**see online supplementary figure 8**), and decreased c-Myc protein half-life (**figure 5E**, lower panel). We then tested whether BVES could regulate c-Myc ubiquitylation, a central post-translational event targeting its destruction. Indeed, by overexpressing BVES we observed increased c-Myc polyubiquitylation (**figure 5F**). Moreover, inhibiting the proteasome using MG132 blocked BVES-induced reduction of c-Myc (**figure 5F**). Hence, our results suggest that BVES promotes the post-translational degradation of c-Myc.

BVES interacts with PR61α, PP2Ac, and c-Myc

To identify a molecular mechanism by which BVES orchestrates c-Myc degradation, we conducted a Y2H screen to define the BVES interactome. Characterization of this interactome using the PANTHER (Protein ANalysis THrough Evolutionary Relationships) Classification System[31] identified a number of biologic processes influenced by BVES (**figure 6A)**. Interestingly, the screen identified that BVES interacted with four of the five members of the B' family of PP2A regulatory subunits (PPP2R5A, PPP2R5B, PPP2R5D, and PPP2R5E). PPP2R5A, also known as PR61α, is a key regulator of PP2A mediated c-Myc dephosphorylation. PR61α directs the heterotrimeric PP2A complex, consisting of a regulatory, catalytic, and structural subunit, to associate with doubly phosphorylated (T58/S62) c-Myc and dephosphorylate

S62, resulting in increased levels of monophosphorylated T58 c-Myc species, which signals c-Myc to be degraded by the proteaosome[32].

The BVES:PR61α interaction was then confirmed by directed Y2H (**figure 6A**) and by exogenous and endogenous co-immunoprecipitation in HEK 293T cells (**figure 6B and C**). If BVES were interacting with PR61α to promote c-Myc degradation, we hypothesized that BVES would complex with both the PP2A catalytic subunit (PP2Ac) and c-Myc, which we then demonstrated by co-immunoprecipitation (**figure 6D and E and see online supplementary figure 9)**. We further used the proximity ligation assay (PLA) and confirmed interaction of both exogenous and endogenous BVES with endogenous PR61α and c-Myc (**figure 6F).** Overall, these data indicate that BVES complexes with c-Myc, PR61α, and the PP2A catalytic subunit.

BVES is essential for PR61α-mediated c-Myc degradation

PP2A dephosphorylation of S62 requires c-Myc to be phosphorylated at residue T58[33]. If BVES reduces c-Myc through PP2A, we reasoned c-Myc^{T58A}, a c-Myc mutant resistant to T58 phosphorylation, would escape BVES-induced degradation. Indeed, BVES expression consistently reduced c-Myc^{WT} but had no effect on c-Myc^{T58A} (**figure 7A**). We next hypothesized that knockdown of BVES would ablate PR61α-PP2A induced c-Myc degradation. Overexpression of PR61α reduced c-Myc protein subtly but consistently as previously reported[32] (**figure 7B**; compare lane 1 and 3). Knocking down BVES, however, rescued PR61α-induced degradation (**figure 7B**; compare lanes 3 and 4). We then tested whether BVES could enhance PR61α-mediated c-Myc degradation, and indeed, overexpression of BVES and PR61α substantially reduced c-Myc protein compared to PR61α or BVES alone (**figure 7C**; compare lane 4 to 2 or 3).

We then sought to determine whether BVES requires PR61α to degrade c-Myc. For these experiments we first mapped the BVES:PR61α interaction domain by serial deletions to the carboxy-terminus of BVES. Deleting the carboxy-terminal 30 residues, but not the last 15 residues, disrupted the BVES:PR61α interaction as demonstrated by Y2H and by co-IP, thus mapping the interaction domain to residues 330-345 (**figure 7D**). Importantly, this uncoupling mutant (BVES-330) demonstrated reduced affinity for c-Myc (**figure 7E**) and was unable to reduce c-Myc levels (**figure 7F**), indicating BVES indeed requires interaction with PR61α to regulate c-Myc. Overall, our results demonstrate that BVES, through PR61α, promotes c-Myc dephosphorylation, destabilization, and destruction, and thus provides mechanistic insight into one manner by which BVES may contribute to inflammatory carcinogenesis.

DISCUSSION

We, and others, have shown that BVES is underexpressed in gastrointestinal cancers and that restoration of BVES in cancer cell lines induces epithelial features. Here we provide the first genetic evidence that BVES modifies cancer phenotypes, as we demonstrate that mice lacking *Bves* have increased tumor multiplicity and dysplasia after establishment of inflammatory carcinogenesis. Further, we show *Bves*$^{-/-}$ tumors have increased c-Myc protein resulting in activation of c-Myc regulated networks. Moreover, we identify that BVES interacts with PR61α, a key regulatory subunit of the PP2A phosphatase complex, and promotes PP2A-mediated c-Myc dephosphorylation leading to c-Myc degradation. Uncoupling the BVES:PR61α interaction blocks BVES-dependent reduction of cellular c-Myc levels. To our knowledge, this is the first junctional-associated protein identified that regulates post-translational c-Myc status. The potential clinical relevance is demonstrated as we observed that *BVES* is downregulated in CAC likely secondary to promoter methylation. However, perhaps more importantly, we establish that the *BVES* promoter is also aberrantly methylated in distant, normal appearing tissues in patients with CAC/HGD—suggesting a field effect. Thus, our findings not only reveal that deletion of BVES promotes CAC, but also that *BVES* promoter methylation status may be a clinically important surrogate marker of colitis-associated dysplasia or CAC in IBD patients.

Chronic colitis has been shown to accelerate genome-wide methylation changes[34]; it has been hypothesized that this greater rate of methylation contributes to the increased cancer risk in patients with colitis by silencing tumor suppressors. Understanding how methylation broadly affects inflammatory tumorigenesis is important to design therapies

and screening strategies for IBD patients. Our report specifically identifies that the *BVES* promoter is hypermethylated in UC patients who have CAC. Interestingly, *BVES* promoter hypermethylation is observed not only in the cancerous tissue, but also in the non-malignant mucosa in these patients. Currently, the standard method of cancer screening in IBD patients, who are at up to a 10-fold elevated risk of developing CAC[1], is surveillance colonoscopy performed with the hope that cancer will be detected at an early, treatable stage. Yet the detection of neoplasia in the colon can be challenging in individuals with IBD, as the lesions are frequently flat and difficult to detect in a background of acute and chronic inflammatory changes. Our data suggest that aberrant *BVES* promoter methylation may be a useful biomarker for the presence of CAC, or even dysplasia, and that measuring *BVES* promoter methylation status could serve as a clinically useful tool to identify patients at risk for colon dysplasia or cancer.

While the molecular pathogenesis of CAC remains incompletely understood, recent work has shown the importance of NF-κB signaling[35], the intestinal microbiota[36], the tumor microenvironment[37], and the innate immune system[38] in regulating inflammatory tumorigenesis. A growing body of evidence also supports the important role of epithelial junctional constituents in inflammation and CRC. For example, mice expressing a dominant negative N-cadherin display disrupted adherens junctions and develop severe inflammation and colitis-associated dysplasia[39]. Likewise, knocking out *Junctional adhesion molecule* (*Jam-A*) results in a dramatic increase in susceptibility to DSS-induced colitis[8]. Here we show that deletion of *Bves*, a tight junction-associated protein, augments inflammatory carcinogenesis. Indeed, loss of BVES appears to increase tumor initiation and progression. We postulate that this is likely due to dual

regulation of Wnt signaling and c-Myc protein degradation. Our results further strengthen the concept that junctional constituents are important regulators of colitis-induced tumor initiation and progression.

In the last decade, BVES has been shown to regulate a variety of cellular processes. For example, a Y2H screen of a mouse heart library identified an interaction between BVES and GEFT, a guanine nucleotide exchange factor[40]. Indeed, it was shown that expression of BVES modulated cell shape and locomotion, thus linking BVES to Rho-family GTPase signaling[40]. BVES has also been shown, via an interaction with ZO-1, to regulate GEF-H1-mediated RhoA activity[11]. More recently, it was reported that BVES plays a regulatory role in cardiac pacemaking through binding of cAMP and interacting with potassium channel TREK-1[41]. Further, BVES interacts with CAV3, a caveolin expressed in the muscle tissue, and cardiac myocytes in *Bves*$^{-/-}$ mice have altered calveolar number and size[42]. Thus, BVES, through scaffolding with protein complexes, regulates a wide variety of basic, yet essential, cellular processes.

Our results now expand the known regulatory roles of BVES to include maintaining appropriate c-Myc protein levels. We show that BVES, through its interaction with the PR61α-containing PP2A phosphatase complex, can promote c-Myc degradation and that silencing BVES prevents PR61α-induced degradation of c-Myc. Moreover, mutating BVES so that it is unable to associate with PR61α renders BVES unable to initiate c-Myc destruction. The post-translational regulation of c-Myc requires coordination of numerous proteins to modify its phosphorylation and ubiquitylation status[21]. Precisely how BVES coordinates the PR61α-PP2A complex remains to be understood, but given that analysis of BVES structure shows no apparent enzymatic

motifs in BVES, it is likely that BVES acts as a scaffold allowing for complex formation, similar to AXIN1[21]. Interestingly, in addition to the membranous staining of the BVES:PR61α complex, there also appears to be peri-nuclear and cytoplasmic localization (**figure 6F**), which is consistent with previous reports describing the dynamic subcellular localization of BVES and its family members[43]. The PP2A family has been associated with tight junctional complexes regulating cellular permeability, but their exact role remains controversial[44]. BVES may bridge PP2A complexes to tight junctions and our report adds a new molecular mechanism for "outside-in" signaling in the epithelium.

Because c-Myc regulates thousands of genes, even subtle changes in c-Myc expression can have profound effects on cellular transcriptomes that promote tumorigenesis[45]. Indeed, strict regulation of c-Myc is an important component of homeostasis, and this is particularly true in the intestine. Acute expression of c-Myc, for example, dramatically expands the intestinal crypts and results in loss of differentiated cells[46]. Moreover, it has been shown that c-Myc is essential for *Apc*-mediated intestinal tumorigenesis[17]. Thus, BVES may serve as an important suppressor of inflammatory tumorigenesis via attenuating excessive c-Myc levels. More broadly, BVES could act as a regulator of c-Myc in a variety of tissues, as BVES is expressed in most epithelial tissues, such as lung, stomach, and breast, and its downregulation or promoter hypermethylation has been documented in diverse epithelium[11–13].

Taking our data together, one can envision a model in which chronic inflammation leads to *BVES* promoter hypermethylation, resulting in suppression of *BVES* transcription and reduced cellular protein levels. Loss of BVES impairs PR61α

directed PP2A dephosphorylation of c-Myc, thus favoring increased cellular pools of c-Myc, a potent oncogene, likely, in cooperation with other oncogenic events, contributing to tumor progression (**figure 8**).

ACKNOWLEDGEMENTS:

We would like to thank the members of the Williams lab who helped discuss and review the manuscript. We would also like to thank Dr. Brian Grieb and Dr. Joseph Roland for their helpful suggestions. Finally, we appreciate the advice and counsel from Dr. R. Daniel Beauchamp and Dr. Barbara Fingelton in preparing the manuscript.

REFERENCES

1. A, Mantovani A, Allavena P, et al. Cancer-related inflammation. Nature 2008;454(7203):436–44.
2. Danese S, Mantovani A. Inflammatory bowel disease and intestinal cancer: a paradigm of the Yin-Yang interplay between inflammation and cancer. Oncogene 2010;29(23):3313–3323.
3. Terzić J, Grivennikov S, Karin E, et al. Inflammation and colon cancer. Gastroenterology 2010;138(6):2101–2114.e5.
4. Jess T, Simonsen J, Jørgensen KT, et al. Decreasing risk of colorectal cancer in patients with inflammatory bowel disease over 30 years. Gastroenterology 2012;143(2):375–81.
5. Schmitz H, Barmeyer C, Fromm M, et al. Altered tight junction structure contributes to the impaired epithelial barrier function in ulcerative colitis. Gastroenterology 1999;116(2):301–309.
6. Gibson P, Rosella O, Nov R, et al. Colonic epithelium is diffusely abnormal in ulcerative colitis and colorectal cancer. Gut 1995;36(6):857–863.
7. Karayiannakis AJ, Syrigos KN, Efstathiou J, et al. Expression of catenins and E-cadherin during epithelial restitution in inflammatory bowel disease. J Pathol 1998;185(4):413–418.
8. Vetrano S, Rescigno M, Rosaria Cera M, et al. Unique role of junctional adhesion molecule-A in maintaining mucosal homeostasis in inflammatory bowel disease. Gastroenterology 2008;135(1):173–184.
9. Severson EA, Parkos CA. Mechanisms of outside-in signaling at the tight junction by junctional adhesion molecule A. Ann N Y Acad Sci 2009;1165:10–18.
10. Orsulic S, Huber O, Aberle H, et al. E-cadherin binding prevents β-catenin nuclear localization and β-catenin / LEF- 1-mediated transactivation. J Cell Sci 1999;1245:1237–1245.
11. Williams CS, Zhang B, Smith JJ, et al. BVES regulates EMT in human corneal and colon cancer cells and is silenced via promoter methylation in human colorectal carcinoma. J Clin Invest 2011;121(10):4056–4069.
12. Feng Q, Hawes SE, Stern JE, et al. DNA methylation in tumor and matched normal tissues from non-small cell lung cancer patients. Cancer Epidemiol Biomarkers Prev 2008;17(3):645–654.

13. Kim M, Jang HR, Haam K, et al. Frequent silencing of popeye domain-containing genes, BVES and POPDC3, is associated with promoter hypermethylation in gastric cancer. Carcinogenesis. 2010;31(9):1685–1693.

14. Toon CW, Chou A, Clarkson A, et al. Immunohistochemistry for Myc predicts survival in colorectal cancer. PLoS One 2014;9(2):e87456.

15. Koo SH, Kwon KC, Shin SY, et al. Genetic alterations of gastric cancer: comparative genomic hybridization and fluorescence in situ hybridization studies. Cancer Genet Cytogenet 2000;117(2):97–103.

16. Cowling VH, Cole MD. E-cadherin repression contributes to c-Myc-induced epithelial cell transformation. Oncogene 2007;26(24):3582–3586.

17. Yekkala K, Baudino TA. Inhibition of intestinal polyposis with reduced angiogenesis in ApcMin/+ mice due to decreases in c-Myc expression. Mol Cancer Res 2007;5(12):1296–1303.

18. Ciclitira PJ, Macartney JC, Evan G. Expression of c-myc in non-malignant and pre-malignant gastrointestinal disorders. J Pathol 1987;151(4):293–296.

19. Brentnall TA, Pan S, Bronner MP, et al. Proteins that underlie neoplastic progression of ulcerative colitis. Proteomics - Clin Appl 2009;3(11):1326–1337.

20. Suzuki R, Miyamoto S, Yasui Y, et al. Global gene expression analysis of the mouse colonic mucosa treated with azoxymethane and dextran sodium sulfate. BMC Cancer 2007;7:84.

21. Arnold HK, Zhang X, Daniel CJ, et al. The Axin1 scaffold protein promotes formation of a degradation complex for c-Myc. EMBO J 2009;28(5):500–512.

22. Barrett CW, Fingleton B, Williams A, et al. MTGR1 is required for tumorigenesis in the murine AOM/DSS colitis-associated carcinoma model. Cancer Res 2011;71(4):1302–1312.

23. Andrée B, Fleige A, Arnold HH, et al. Mouse Pop1 is required for muscle regeneration in adult skeletal muscle. Mol Cell Biol 2002;22(5):1504–1512.

24. Wang F, Flanagan J, Su N, et al. RNAscope: A novel in situ RNA analysis platform for formalin-fixed, paraffin-embedded tissues. J Mol Diagnostics 2012;14(1):22–29.

25. Weber CR, Nalle SC, Tretiakova M, et al. Claudin-1 and claudin-2 expression is elevated in inflammatory bowel disease and may contribute to early neoplastic transformation. Lab Invest 2008;88(10):1110–1120.

26. Korinek V, Barker N, Morin PJ, et al. Constitutive transcriptional activation by a beta-catenin-Tcf complex in APC-/- colon carcinoma. Science 1997;275(5307):1784–1787.

27. Kohno H, Suzuki R, Sugie S, et al. B-catenin mutations in a mouse model of inflammation-related colon carcinogenesis induced by 1,2-dimethylhydrazine and dextran sodium sulfate. Cancer Sci 2005;96(2):69–76.

28. Krämer A, Green J, Pollard J, et al. Causal analysis approaches in Ingenuity Pathway Analysis. Bioinformatics 2014;30 (4): 523-530.

29. Tetsu O, McCormick F. Beta-catenin regulates expression of cyclin D1 in colon carcinoma cells. Nature 1999;398(6726):422–426.

30. Mann B, Gelos M, Siedow Q, et al. Target genes of beta-catenin-T cell-factor/lymphoid-enhancer-factor signaling in human colorectal carcinomas. Proc Natl Acad Sci U S A 1999;96(4):1603–1608.

31. Mi H, Muruganujan A, Thomas PD. PANTHER in 2013: Modeling the evolution of gene function, and other gene attributes, in the context of phylogenetic trees. Nucleic Acids Res 2013;41(D1):D377–86.

32. Arnold HK, Sears RC. Protein Phosphatase 2A regulatory subunit B56α associates with c-Myc and negatively regulates c-Myc accumulation protein. Mol Cell Biol 2006;26(7):2832–2844.

33. Yeh E, Cunningham M, Arnold H, et al. A signalling pathway controlling c-Myc degradation that impacts oncogenic transformation of human cells. Nat Cell Biol 2004;6(4):308–318.

34. Issa JJ, Ahuja N, Toyota M. Accelerated age-related CpG island methylation in ulcerative colitis. Cancer Res 2001:3573–3577.

35. Grivennikov S, Karin E, Terzic J, et al. IL-6 and Stat3 are required for survival of intestinal epithelial cells and development of colitis-associated cancer. Cancer Cell 2009;15(2):103–113.

36. Arthur JC, Perez-Chanona F, Muhlbauger M, et al. Intestinal inflammation targets cancer-inducing actvity of the microbiota. Science 2012; 338 (6103); 120-123.

37. Katoh H, Wang D, Daikoku T, et al. CXCR2-expressing myeloid-derived suppressor cells are essential to promote colitis-associated tumorigenesis. Cancer Cell 2013;24(5):631–644.

38. Fukata M, Chen A, Vamadevan AS, et al. Toll-like receptor-4 promotes the development of colitis-associated colorectal tumors. Gastroenterology 2007;133(6):1869–81.

39. Hermiston ML, Gordon JI. Inflammatory bowel disease and adenomas in mice expressing a dominant negative N-Cadherin. Science 1995;270(5239):1203–1207.

40. Smith TK, Hager H, Francis R, et al. Bves directly interacts with GEFT, and controls cell shape and movement through regulation fo Rac1/Cdc42 activity. Proc Natl Acad Sci U S A 2008;105(24): 8298-8303.

41. Froese A, Breher SS, Waldeyer C, et al. Popeye domain containin proteins are essential for stress-mediated modulation of cardiac pacemaking in mice. J Clin Invest 2012;122(3):1119-1130.

42. Alcalay Y, Hochhauser E, Kliminski V, et al. Popeye domain containing 1 (Popdc1/Bves) is a caveolae-associated protein involved in ischemia tolerance. PLoS One 2013;8(9):e71100.

43. Osler ME, Chang MS, Bader DM. Bves modulates epithelial integrity through an interaction at the tight junction. J Cell Sci 2005;118(20):4667–4678.

44. Dunagan M, Chaudhry K, Samak G, et al. Acetaldehyde disrupts tight junctions in Caco-2 cell monolayers by a protein phosphatase 2A-dependent mechanism. AJP Gastrointest Liver Physiol 2012;303(12):G1356–64.

45. Kim J, Woo AJ, Chu J, et al. A Myc network accounts for similarities between embryonic stem and cancer cell transcription programs. Cell 2010;143(2):313–324.

46. Finch AJ, Soucek L, Junttila MR, et al. Acute overexpression of Myc in intestinal epithelium recapitulates some but not all the changes elicited by Wnt/beta-catenin pathway activation. Mol Cell Biol 2009;29(19):5306–5315.

Legends

Figure 1 A field effect of *BVES* promoter hypermethylation in colitis-associated cancer.

(A) Average *BVES* promoter methylation status in the indicated sample from the Infinium HumanMethylation 450 Array. Methylation was measured in four sample types: colon epithelia from patients who did not have UC (Control—No UC); colon epithelia from UC patients who did not have dysplasia or carcinoma (UC—no HGD/CAC); non-malignant colon epithelia from UC patients (UC—concurrent HGD/CAC) and malignant colon epithelia (HGD/CAC) from UC patients who had dysplasia/carcinoma. Control—No UC, n=17; UC—no HGD/CAC, n=11; UC—concurrent HGD/CAC, n=10; HGD/CAC, n=10. **p<0.01.

(B) Pyrosequencing at four sequential CpG dinucleotides in the *BVES* promoter. Each shape represents a separate individual, with mean methylation values depicted with black bars. ***p<0.001.

(C) Representative images of high-resolution in situ (RNAscope™) analysis of *BVES* message in normal colons (n=11), UC (n=13), and CAC (n=19). Right: Quantification of *BVES* expressing epithelial cells per tissue microarray core. Size standard=50 microns. ***p<0.001

Figure 2 BVES modifies inflammatory carcinogenesis.

(A) Schematic of AOM/DSS protocol and timeline. Mice were injected with 7.5 mg/kg of AOM and treated with 2.5% DSS at the indicated time.

(B) Left: Heat map of RNA-seq data derived from WT colons (n=3) and WT AOM/DSS tumors (n=3). Red indicates genes increased and green indicates genes decreased in

tumors compared to normal colon. Right: qPCR of *Bves* message levels in normal colons (Normal, n=5), non-malignant AOM/DSS treated colon (NM, n=5) and AOM/DSS tumor (Tumor, n=6). Tissue harvested from WT mice after AOM/DSS treatment. ***p<0.001.

(C) Weights of *Bves*$^{-/-}$ and WT mice during AOM/DSS treatment. Weights are presented as fraction of initial weight. *Bves*$^{-/-}$ (male: n=8, female: n=7) and WT (male: n=5, female: n=10). *p<0.05, ***p<0.01, ***p<0.001.

(D) Representative colonoscopy images of WT and *Bves*$^{-/-}$ colons after the second cycle of DSS treatment. Right: Quantification of tumor multiplicity by endoscopy assessment.

(E) Tumor incidence, multiplicity, and size distribution at necropsy in WT and *Bves*$^{-/-}$ mice. Blue = female mice, black = male mice.*p<0.05, ***p<0.001.

(F) Left: Representative H&E stained sections demonstrating the histologic features of WT and *Bves*$^{-/-}$ tumors. Size standard=100 microns. Right: Blinded histological scoring of degree of dysplasia of tumors from WT and *Bves*$^{-/-}$ mice. Graph represents percentage of mice with intratumoral low or high-grade dysplasia.

Figure 3 Dysregulated Wnt signaling in *Bves*$^{-/-}$ tumors.

(A) Left: Representative images of phospho-histone H3 (pH3) immunohistochemistry in WT and *Bves*$^{-/-}$ tumors. Size standard=50 microns. Right: Quantification of pH3 positive cells per tumor high power field (HPF). Data is presented as the mean number of positive cells per tumor HPF per mouse. At least five HPF per mouse were scored. Student's t test, *p<0.05.

(B) Left: H&E stained sections, size standard=50 microns. Middle: Representative images of β-catenin immunohistochemistry, low magnification, size standard=50

microns. Right: β-catenin immunohistochemistry, high magnification, size standard=20 microns. Far right: Quantification of intratumoral β-catenin immunohistochemistry. An index was employed to quantify extent of nuclear and cytoplasmic β-catenin staining. This index is generated by multiplying the staining intensity (on a scale of 100-500) by percentage of the cells demonstrating nuclear staining. For example, a score of 500 indicates a field that demonstrated very intense nuclear β-catenin stain while a score of 100 indicates a field that has weak nuclear β-catenin staining. Data is presented as the mean score per tumor HPF per mouse. At least five HPF per mouse were scored.

(C) Wnt target genes upregulated in *Bves*$^{-/-}$ tumors identified in RNA-seq dataset (WT, n=3; *Bves*$^{-/-}$, n=3).

(D) Immunoblot of Cyclin D1 and c-jun in *Bves*$^{-/-}$ and WT tumors. β-actin was used as a loading control.

Figure 4 c-Myc signaling is dysregulated in *Bves*$^{-/-}$ mice in inflammatory carcinogenesis. (A) Left: Representative images of immunohistochemistry for intratumoral c-Myc. Right: quantification of c-Myc positive cells per tumor high power field (HPF). HPFs were scored according to an index from 1-4 (a score of 1 denotes less than 25% of positive cells per HPF; a score of 2 denotes 25-50%; a score of 3 denotes 50-75%; a score of 4 denotes 80-100%). Data is presented as the mean score per tumor HPF per mouse. At least five HPF per mouse were scored. Student's t test, *$p<0.05$. Size standard=50 microns

(B) Immunoblot of c-Myc in WT and *Bves*$^{-/-}$ normal adjacent colons. Blots were imaged using the LiCor Odyssey system and quantified using Image Studio analysis. Student's t test, $p<0.05$.

(C) Immunoblot of c-Myc in WT (n=3) and *Bves*$^{-/-}$ (n=3) intestinal crypts.

(D) qPCR for *Odc* and *E2f2* in enteroid cultures Student's t test, *$p<0.05$.

In all western blots, β-actin served as loading control.

Figure 5 BVES regulates c-Myc stability and activity.

(A) c-Myc and T58 phospho-c-Myc protein levels after *BVES* knockdown in HEK 293T (left) or Caco2 (right) cells after 48 hr serum starvation.

(B) qRT-PCR assay for c-Myc targets *ODC* and *CAD* following *BVES* knockdown in the indicated cell lines. Data are presented as mean ±SEM and in triplicates. *$p<0.05$, **$p<0.01$.

(C) Cycloheximide treatment (100 μg/ml) of HEK 293T cells with and without *Bves* knockdown followed by immunoblotting for c-Myc.

(D) c-Myc and T58 phospho-c-Myc protein levels after overexpression of V5:BVES in HEK 293T cells.

(E) HEK 293T cells co-transfected with HA:c-Myc and V5:BVES were then treated with cycloheximide (100 μg/ml) followed by immunoblotting for the indicated protein.

(F) Left: His:Ubiquitin and HA:c-Myc were co-transfected into HEK 293T cells along with V5:BVES. Cells were treated with proteasome inhibitor MG132 (20 μm) for 4 hours before His:Ubiquitin complexes were immunoprecipitated and resolved by SDS-PAGE. Ubiquitylated HA:c-Myc complexes were visualized by immunoblotting (Ub-c-Myc). Total ubiquitylated protein (Total ub) was examined as a control. Right: HEK 293T cells

co-transfected with HA:c-Myc and V5:BVES were treated with proteasome inhibitor MG132 (20 μm) for 4 hours. Whole cell lysates were analyzed for HA:c-Myc expression. In all immunoblots, β-actin was used as a loading control. All experiments were replicated three times.

Figure 6 BVES interacts with PR61α, PP2A, and c-Myc.

(A) PANTHER Biologic Process Analysis of BVES interactome. Inset: Directed yeast two-hybrid of BVES and PR61α.

(B) Co-immunoprecipitation of exogenous and (**C**) endogenous PR61α:BVES complexes in HEK 293T cells.

(D) Co-immunoprecipitation of V5:BVES and HA:PP2Ac or (**E**) HA:c-Myc.

(F) Left: Proximity ligation assay in HEK 293T cells transfected with V5:BVES. Left: control, middle: α-PR61α, right: α-c-Myc. Right: Proximity ligation assay in HEK 293T cells for endogenous protein interactions. Left: control, middle: α-PR61α, right: α-c-Myc. Anti-HA was used as a control in both exogenous and endogenous localization. Scale bar denotes 10 μm. Red staining is positive signal from the PLA interaction, and blue staining is DAPI. In all immunoblots blots, β-actin was used to ensure loading consistency. All experiments were repeated at least two times.

Figure 7 The BVES:PR61α interaction is required to promote c-Myc degradation.

(A) WT HA:c-Myc or phospho-mutant HA:T58A c-Myc levels after either empty vector (negative control) or V5:BVES transfection in HEK 293T cells.

(B) Immunoblotting for HA:c-Myc levels following PR61α overexpression in the setting of BVES knockdown or (**C**) when both PR61α and BVES are present HEK 293T cells. **(D)** Top: Mapping the PR61α BVES binding interface via directed yeast two-hybrid (Full length BVES, residues 1-345, 1-330, 1-302, negative control (Neg Ctrl), and positive control (Pos Ctrl)). Below: Co-immunoprecipitation of the indicated BVES mutants and PR61α in HEK 293T cells..

(**E**) Co-immunoprecipitation of the indicated BVES mutants and HA:c-Myc in HEK 293T cells.

(F) HA:c-Myc protein levels after transfection of the indicated BVES construct in HEK 293T cells.

In all immunoblots, β-actin was used as a loading control. All experiments were repeated at least two times.

Figure 8 Working model of the role of BVES in regulating c-Myc degradation and colitis-associated cancer development.